

Air Force Institute of Technology

AFIT Scholar

Theses and Dissertations

Student Graduate Works

3-17-2008

Optimal Guidance of a Relay MAV for ISR Support Beyond Line-of-Sight

John H. Hansen

Follow this and additional works at: <https://scholar.afit.edu/etd>



Part of the [Hardware Systems Commons](#), and the [Systems Engineering and Multidisciplinary Design Optimization Commons](#)

Recommended Citation

Hansen, John H., "Optimal Guidance of a Relay MAV for ISR Support Beyond Line-of-Sight" (2008). *Theses and Dissertations*. 2728.

<https://scholar.afit.edu/etd/2728>

This Thesis is brought to you for free and open access by the Student Graduate Works at AFIT Scholar. It has been accepted for inclusion in Theses and Dissertations by an authorized administrator of AFIT Scholar. For more information, please contact richard.mansfield@afit.edu.



OPTIMAL GUIDANCE OF A RELAY MAV FOR ISR

SUPPORT BEYOND LINE-OF-SIGHT

THESIS

John H. Hansen, Second Lieutenant, USAF
AFIT/GAE/ENG/08-01

**DEPARTMENT OF THE AIR FORCE
AIR UNIVERSITY**

AIR FORCE INSTITUTE OF TECHNOLOGY

Wright-Patterson Air Force Base, Ohio

APPROVED FOR PUBLIC RELEASE; DISTRIBUTION UNLIMITED

The views expressed in this thesis are those of the author and do not reflect the official policy or position of the United States Air Force, Department of Defense, or the United States Government.

AFIT/GAE/ENG/08-01

**OPTIMAL GUIDANCE OF A RELAY MAV FOR ISR
SUPPORT BEYOND LINE-OF-SIGHT**

THESIS

Presented to the Faculty

Department of Electrical and Computer Engineering

Graduate School of Engineering and Management

Air Force Institute of Technology

Air University

Air Education and Training Command

In Partial Fulfillment of the Requirements for the
Degree of Master of Science in Aeronautical Engineering

John H. Hansen, BS

Second Lieutenant, USAF

March 2008

APPROVED FOR PUBLIC RELEASE; DISTRIBUTION UNLIMITED.

**OPTIMAL GUIDANCE OF A RELAY MAV FOR ISR
SUPPORT BEYOND LINE-OF-SIGHT**

John H. Hansen, BS
Second Lieutenant, USAF

Approved:



Dr. Meir Pachter (Chairman)

March 13, 2008

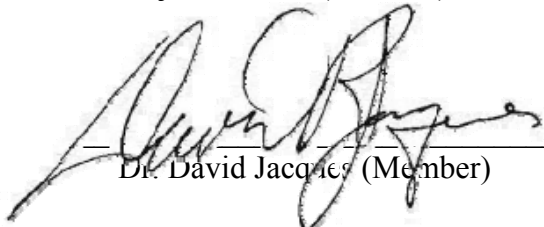
Date



Maj. Paul Blue (Member)

17 Mar 08

Date



Dr. David Jacques (Member)

14 MAR 08

Date

Abstract

This thesis developed guidance laws to optimally position a relay Micro-UAV (MAV) to provide an operator with real-time Intelligence, Surveillance, and Reconnaissance (ISR) by relaying communication and video signals when there is no line-of-sight between the operator at the base and the rover MAV performing the ISR mission.

The ISR system consists of two MAVs, the Relay and the Rover, and a Base. The Relay strives to position itself to minimize the radio frequency (RF) power required for maintaining communications between the Rover and the Base, while the Rover performs the ISR mission, which may maximize the required RF power. The optimal control of the Relay MAV then entails the solution of a differential game. Applying Pontryagin's Maximum Principle yields a nonlinear Two-Point Boundary Value Problem (TPBVP).

Suboptimal solutions are also analyzed to aid in solving the TPBVP which yields the solution of the differential game. One suboptimal approach is based upon the geometry of the ISR system. Another suboptimal approach envisions a stationary Rover and solves for the optimal path for the Relay. Both suboptimal approaches showed that the optimal path for the Relay is to head straight toward the midpoint between the Rover and the Base.

Acknowledgements

I would first like to thank Dr. Meir Pachter, whose support and advisement helped me to accomplish this feat. He helped me to understand more about optimization and its application to differential games. His encouragement to prepare presentations and short papers early helped me to excel in the end.

I would also like to thank Major Paul Blue, who gave me my foundation in optimal control theory. He was never too busy to stop and help me with any questions I had. Special thanks are due to Dr. David Jacques, Dr. Richard Cobb, Don Smith and the entire Fleeting Target team: Greg, Doug, Nate and Troy. We've all worked together to build this system and it's been fun.

I would also like to thank my parents, whose constant support and love throughout the years have always helped me strive to do my best.

My deepest thanks are reserved for my dear wife and son. Your patience and support have always inspired me to work hard, especially during those times when I was not very motivated. I love you and am truly grateful for your unending love and the eternal joy that we share as a family. Lastly, I thank my Father in Heaven who has blessed me with such wonderful friends and family.

John H. Hansen

Table of Contents

	Page
Abstract.....	iv
Acknowledgements.....	v
List of Figures.....	viii
List of Symbols.....	x
List of Abbreviations	xi
1 Introduction.....	1
1.1 Operational Background.....	1
1.2 Problem Statement.....	2
1.3 Thesis Purpose	2
1.4 Thesis Outline.....	3
2 Background.....	4
2.1 Motivation.....	4
2.2 Related Research	4
2.3 Research Statement.....	5
3 Theoretical Analysis	6
3.1 System Definition.....	6
3.2 Suboptimal Approaches.....	10
3.2.1 Geometric Approach.....	10
3.2.2 One-Sided Optimization	13
3.2.3 Suboptimal Solution Applied to TPBVP	15
3.3 Planning Horizon	17
4 Demonstration Hardware and Testing	22
4.1 Demonstration Configuration	22

	Page
4.1.1 Unmanned Aircraft	22
4.1.2 Autopilot	22
4.1.3 Communications Transmission.....	23
4.1.4 Sensor Data Transmission.....	24
4.1.5 Relay Configuration.....	24
4.1.6 Implementation of Relay MAV Guidance.....	25
4.2 Testing Procedure	26
5 Results and Analysis	27
5.1 Numerical Results.....	27
5.1.1 Suboptimal Geometric Results	27
5.1.2 One-Sided Optimization Results.....	31
5.1.3 Results Using Complete System.....	34
5.2 Test Results.....	40
6 Conclusions and Recommendations	41
6.1 Conclusions.....	41
6.2 Recommendations.....	42
Appendix A – Geometry.....	43
Appendix B – Static Optimization Approach	45
Appendix C – Practical Relay Guidance Code	47
Bibliography	48

List of Figures

		Page
Figure 1:	Schematic of Relay System	7
Figure 2:	Schematic of Relay System Showing the Midpoint	10
Figure 3:	Schematic of Relay System Showing Isocost Circle	11
Figure 4:	Motion of M and O Forms Similar Triangles	12
Figure 5:	Flow Chart of Matlab Programs Which Produce Full System Results.....	17
Figure 6:	Schematic of Initial Condition Border Line.....	18
Figure 7:	Initial Condition with Limited Planning Horizon.....	18
Figure 8:	Initial Condition with Unlimited Planning Horizon	19
Figure 9:	Schematic of Relay Location Closest to Base	20
Figure 10:	Sig Rascal 110 (©2008 Tower Hobbies).....	22
Figure 11:	Kestrel Autopilot System (©2008 Procerus Technologies).....	23
Figure 12:	Xtend OEF RF Module (©2007 Digi International).....	24
Figure 13:	Black Widow 1 W Transmitter and Receiver Set (©2007 Black Widow AV)	24
Figure 14:	Setup for Sensor Data Relay Demonstration	25
Figure 15:	Detail of Setup for Sensor Data Relay Demonstration	25
Figure 16:	Geometric Time History for $T = 0.25$, $\alpha = 1$, $r_{E_0} = 0.5$, and $\theta_0 = \frac{\pi}{6}$	27
Figure 17:	Geometric Spatial Results for $T = 0.25$, $\alpha = 1$, $r_{E_0} = 0.5$, and $\theta_0 = \frac{\pi}{6}$	28
Figure 18:	Geometric Time History for $T = 0.48$, $\alpha = 1$, $r_{E_0} = 0.5$, and $\theta_0 = \frac{\pi}{3}$	28
Figure 19:	Geometric Spatial Results for $T = 0.48$, $\alpha = 1$, $r_{E_0} = 0.5$, and $\theta_0 = \frac{\pi}{3}$	29
Figure 20:	Geometric Time History for $T = 0.5$, $\alpha = 2$, $r_{E_0} = 0.5$, and $\theta_0 = \frac{\pi}{6}$	30
Figure 21:	Geometric Spatial Results for $T = 0.5$, $\alpha = 2$, $r_{E_0} = 0.5$, and $\theta_0 = \frac{\pi}{6}$	30

	Page
Figure 22: One-Sided Time History for $T = 0.25$, $r_{E_0} = 0.5$, and $\theta_0 = \frac{\pi}{6}$	31
Figure 23: One-Sided Spatial Results for $T = 0.25$, $r_{E_0} = 0.5$, and $\theta_0 = \frac{\pi}{6}$	32
Figure 24: One-Sided Time History for $T = 0.48$, $r_{E_0} = 0.5$, and $\theta_0 = \frac{\pi}{3}$	33
Figure 25: One-Sided Spatial Results for $T = 0.48$, $r_{E_0} = 0.5$, and $\theta_0 = \frac{\pi}{3}$	33
Figure 26: Full System Time History for $T = 0.25$, $\alpha = 1$, $r_{E_0} = 0.5$ and $\theta_0 = \frac{\pi}{6}$	35
Figure 27: Comparative Spatial Results for $T = 0.25$, $\alpha = 1$, $r_{E_0} = 0.5$ and $\theta_0 = \frac{\pi}{6}$	36
Figure 28: Full System Time History for $T = 0.48$, $\alpha = 1$, $r_{E_0} = 0.5$ and $\theta_0 = \frac{\pi}{3}$	37
Figure 29: Comparative Spatial Results for $T = 0.48$, $\alpha = 1$, $r_{E_0} = 0.5$ and $\theta_0 = \frac{\pi}{3}$	38
Figure 30: Full System Time History for $T = 0.5$, $\alpha = 2$, $r_{E_0} = 0.5$, and $\theta_0 = \frac{\pi}{6}$	39
Figure 31: Comparative Spatial Results for $T = 0.5$, $\alpha = 2$, $r_{E_0} = 0.5$, and $\theta_0 = \frac{\pi}{6}$...	40
Figure 32: Schematic of Fixed Points Showing Isocost Circle	43

List of Symbols

B	=	Base
E	=	Relay MAV
E_c	=	Relay Location Closest to Base Along Optimal Guidance Path
\mathcal{H}	=	Hamiltonian Equation of System
M	=	Midpoint Between Rover and Base
O	=	Rover MAV
r_E	=	Distance of Relay MAV from Base
r_O	=	Distance of Rover MAV from Base
T	=	Time Planning Horizon of Algorithm
T_c	=	Conjugate Time Planning Horizon
V_E	=	Velocity of Relay
V_O	=	Velocity of Rover
x	=	General Reference to All States of a System
X_0	=	Initial Value of Parameter X
X_k	=	Value of Parameter X for Iteration Step k
\mathcal{Y}	=	Objective Cost
α	=	Non-Dimensional Speed Ratio ($\alpha = V_O/V_E$)
θ	=	Included Angle of the Radials From the Base to the Relay and the Rover
λ	=	General Reference to All Co-States of a System
λ_X	=	Co-State of State X
φ	=	Course Angle of Rover
ψ	=	Course Angle of Relay

List of Abbreviations

AFIT	Air Force Institute of Technology
ANT	Advanced Navigation Technology
AUGNet	Ad-hoc UAV Ground Network
ISR	Intelligence, Surveillance and Reconnaissance
KKT	Karush, Kuhn, Tucker
LOS	Line-Of-Sight
MAV	Micro Aerial Vehicle
NLOS	Near Line-Of-Sight
RF	Radio Frequency
TPBVP	Two-Point Boundary Value Problem
UAV	Unmanned Aerial Vehicle

OPTIMAL GUIDANCE OF A RELAY MAV FOR ISR SUPPORT BEYOND LINE-OF-SIGHT

1 Introduction

1.1 *Operational Background*

Lessons learned from OPERATION ENDURING FREEDOM and OPERATION IRAQI FREEDOM have demonstrated a need for teams on the ground in urban environments to organically engage high value, time-sensitive targets in real-time, from Near Line-of-Sight (NLOS) ranges (500 m to 5 km) without waiting for outside air support. Currently, engaging these NLOS targets requires coordination of orbiting assets such as fighter or bomber aircraft, Hellfire missile equipped Predator Unmanned Aerial Vehicles (UAVs), or joint ground-based artillery systems. While devastatingly effective, these systems have three drawbacks: (1) they must be on-station and available for tasking at the time of the request, (2) they have a high probability of causing significant collateral damage, and (3) it takes time to pass the target information and receive clearance to engage the target—an unacceptable delay when engaging a fleeting, high value target.

These drawbacks have led to research in the areas of man-portable Micro Aerial Vehicles (MAVs) which can be deployed by members on location, requiring minimal deployment time and minimal outside coordination. The thesis described herein is therefore the progeny of the Air Force Institute of Technology's (AFIT's) response to the need of such a system. This thesis is the culmination of the theoretical work of several other groups, the implementation of some previous ideas as well as design and integration of new methodologies determined as best suited for completion of the task of creating a miniature, mobile system which can track and engage a moving target.

1.2 Problem Statement

Current man-portable weapon systems require the operator to have unobstructed Line of Sight (LOS) to the target at effective ranges less than 1000 meters. Maintaining an unobstructed LOS in an urban environment, while staying behind protective cover, is challenging at best. These current weapon systems also require the operator to partially expose themselves, both giving away their location and exposing them to enemy fire. In addition, these weapons are essentially large, explosive bullets with no loiter or wait capability. With the current capability, a team tasked with engaging a time sensitive target in a small city would have to infiltrate the city undetected to within approximately 200 meters of the target. Assuming the ground team stayed covert while moving to intercept the target, detection is almost assured once the current weapon systems are used to engage the target. Given their distance from friendly forces, the survivability of the engaging team at this point would be very low. Further, if the target moves, or the ground force team is re-directed, their response time is comparably higher than other systems due to the team's need to stay covert while navigating through an urban environment.

The desired organic capability is a responsive, man-portable, self-propelled, low signature, expendable delivery system with loiter capability, and a NLOS range greater than that currently provided by fielded systems. This new system would allow the user to covertly launch, loiter, track, positively identify, and engage a time-sensitive, high value target from a safe distance. The system should be effective in urban environments as well as desert, maritime, and temperate environments.

1.3 Thesis Purpose

This thesis concentrates on providing reliable communications throughout all phases of the Intelligence, Surveillance, and Reconnaissance (ISR) and engagement

mission by introducing an additional MAV which will act as a relay between the ground team and the envisioned delivery system. The presence of this relay MAV should not increase the operator workload and should therefore fly autonomously to maintain the communication link. The thesis focuses on developing the guidance laws which will dictate the behavior of the relay MAV.

1.4 Thesis Outline

With an established thesis purpose, the remainder of the thesis will now focus on describing the methodology for specifying and validating the developed system. The *Background* chapter provides the problem background, motivation, and an overview of related research work in the fields of communication relays and dynamic games. The *Theoretical Analysis* chapter defines the full dynamic system and several lower-order systems. The *Demonstration Hardware and Testing* chapter describes the hardware components and flight tests associated with proving the theoretical concept of communication relay. The *Results and Analysis* chapter verifies that the developed system meets specified requirements and validates the system using simulation and test results. Finally, the *Conclusions and Recommendations* chapter discusses lessons learned and recommends areas for future research.

2 Background

2.1 *Motivation*

Reliable communication is essential in order to perform the ISR and engage mission. The envisioned man-portable system will not be supported by satellite communications, but will use radio frequency (RF) modems. High frequency radio communications are limited by an adequate Line-Of-Sight (LOS) between the operator at the Base and the MAV. The MAV systems considered in this thesis are utilized to seek out and engage high value targets and will be referred to as Rovers.

There are a number of environments (e.g., urban, forest, mountainous) in which the Base may often lose communication with deployed Rovers because it is not possible to maintain LOS with the Rovers. This thesis focuses on developing guidance laws to optimally position a specialized Relay MAV to provide the operator at the Base with real-time information by relaying communication and sensor data when there is no LOS between the operator and the Rover.

2.2 *Related Research*

Recent studies have produced two general designs for a reliable and robust communication network utilizing mobile communication nodes. The first design consists of one or more mobile communication nodes which form a single chain to relay information between the source and the destination. This is referred to as a “single-flow network.” Many designs for single-flow networks use a fixed source and fixed destination, though they do not discount the possibility of a mobile destination (Dixon and Frew, 2007; Goldenberg et al., 2004). The second design consists of multiple mobile communication nodes which form a “mesh-like network”. This configuration adds fault-

tolerance for a more robust network (Basu and Redi, 2004; Floreano et al., 2007). However, a “mesh-like network” would be ill suited for the envisioned ISR and engagement system due to desired unit covertness while engaging a high value target. In this respect, Brown et al. have developed the Ad-hoc UAV Ground Network (AUGNet) test bed, showing the practicality of UAV-based mobile communication nodes using IEEE 802.11b wireless routers (Brown et al., 2004). The proposed ISR and engagement system may have a network design similar to AUGNet but the Relay must still have an optimal mobility control law in order to optimize network communications.

Dixon and Frew have utilized the AUGNet system with an extremum seeking controller to study cooperative electronic chaining while maximizing the signal-to-noise ratio between the nodes of the multi-hop network (Dixon and Frew, 2007). Goldenberg et al. have shown that communication nodes should be evenly spaced on the line between the source and destination in order to minimize the energy cost of communicating between the two (Goldenberg et al., 2004).

2.3 Research Statement

The main distinction of this work is that no cooperation between the Rover and the Relay is imposed while optimally positioning the communication node (the Relay). This scenario is then modeled by posing a differential game: The Relay strives to position itself such that the RF power required for maintaining communications is minimized, whereas the Rover strives to position itself such that the RF power is maximized. Suboptimal Relay and Rover strategies are provided. These will serve as a first guess in solving the Two-Point Boundary Value Problem (TPBVP) given by the Pontryagin Maximum Principle and which yields the optimal strategies.

3 Theoretical Analysis

3.1 System Definition

It is assumed that the rElay (E) MAV is cognizant of the rOver's (O) instantaneous position relative to the Base (B) as well as its own position. As far as the RF power requirements are concerned, this is determined by their distance from the Base and the Rover-Relay separation. Thus, the state is the distance r_E of the Relay from the Base, the distance r_O of the Rover to the Base, and the angle θ included between the radials from the Base to the Relay and the Rover. This angle is measured clockwise (see Figure 1). The MAVs have simple motion. The control for each MAV is its relative heading angle measured clock-wise from its radial from the Base. Figure 1 provides a visualization of the kinematics. The differential equations of motion are

$$\left. \begin{aligned} \dot{r}_E &= V_E \cos \varphi & , r_E(0) &= r_{E_0} \\ \dot{r}_O &= V_O \cos \psi & , r_O(0) &= r_{O_0} \\ \dot{\theta} &= \frac{1}{r_O} V_O \sin \psi - \frac{1}{r_E} V_E \sin \varphi & , \theta(0) &= \theta_0, 0 \leq t \leq T \end{aligned} \right\} \quad (1)$$

T is the planning horizon utilized by the control algorithm. The cost functional is indicative of the RF power required and is the time averaged sum of the squares of the distance between the Relay and the Rover and between the Relay and the Base:

$$\mathbf{y} = \int_0^T \left(\overline{EO}^2(t) + \overline{BE}^2(t) \right) dt$$

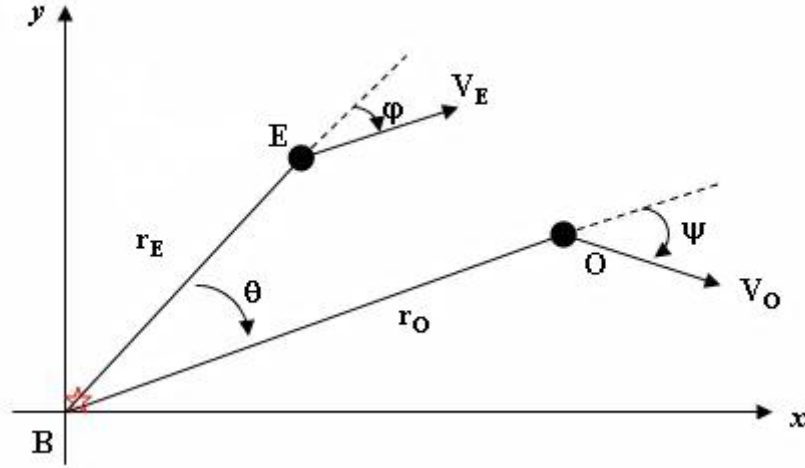


Figure 1: Schematic of Relay System

The points E , B and O in \mathbb{R}^2 represent the positions of the Relay, Base and Rover, respectively. These three points form a triangle which can be utilized to calculate the distance \overline{EO} by the law of cosines.

$$\overline{EO}^2(t) = r_E^2 + r_O^2 - 2r_E r_O \cos \theta$$

Hence the cost functional is

$$y = \int_0^T (2r_E^2 + r_O^2 - 2r_E r_O \cos \theta) dt \quad (2)$$

The relay's objective is to minimize the average RF power required for maintaining communications. The control available to accomplish this task is limited to setting the course angle φ of the Relay, while the Rover does whatever it wants, namely, it performs the ISR mission: in a worst case scenario, one might assume that the Rover is working to maximize the cost functional. The optimization problem is then a differential game where the Relay's control is its relative heading φ and the Rover's control is its relative heading ψ .

The system is analyzed by first non-dimensionalizing the states and the parameters. The velocities are scaled by the velocity of the Relay (V_E), yielding a non-

dimensional speed ratio α ($\alpha = \frac{V_o}{V_E}$). The distances are scaled by the initial distance of the Rover from the Base so that each distance throughout the time history of this ISR mission is measured in units of r_{o_0} . Using these non-dimensional parameters, the differential game in $\mathbb{R}^2 \times \mathbb{S}^1$ now becomes

$$\left. \begin{aligned} \min_{\varphi} \max_{\psi} \mathcal{Y} &= \int_0^T (2r_E^2 + r_o^2 - 2r_E r_o \cos \theta) dt \\ \text{s.t.} \\ \dot{r}_E &= \cos \varphi, \quad r_E(0) = r_{E_0} \\ \dot{r}_o &= \alpha \cos \psi, \quad r_o(0) = 1 \\ \dot{\theta} &= \frac{1}{r_o} \alpha \sin \psi - \frac{1}{r_E} \sin \varphi, \quad \theta(0) = \theta_0, \quad 0 \leq t \leq T \end{aligned} \right\} \quad (3)$$

where the problem parameter is the speed ratio $\alpha \geq 0$. To solve the differential game, the Hamiltonian is introduced in Equation (4)

$$\mathfrak{H} = -2r_E^2 - r_o^2 + 2r_E r_o \cos \theta + \lambda_{r_E} \cos \varphi + \lambda_{r_o} \alpha \cos \psi + \lambda_{\theta} \left(\frac{1}{r_o} \alpha \sin \psi - \frac{1}{r_E} \sin \varphi \right) \quad (4)$$

where λ_{r_E} , λ_{r_o} and λ_{θ} are the system co-states.

According to the Pontryagin Maximum Principle (Pontryagin et al., 1962), the differential equations for the co-states are

$$\left. \begin{aligned} \dot{\lambda}_{r_E} &= 4r_E - 2r_o \cos \theta - \frac{\lambda_{\theta} \sin \varphi}{r_E^2}, \quad \lambda_{r_E}(T) = 0 \\ \dot{\lambda}_{r_o} &= 2r_o - 2r_E \cos \theta + \frac{\lambda_{\theta} \alpha \sin \psi}{r_o^2}, \quad \lambda_{r_o}(T) = 0 \\ \dot{\lambda}_{\theta} &= 2r_E r_o \sin \theta, \quad \lambda_{\theta}(T) = 0 \end{aligned} \right\} \quad (5)$$

and the optimality condition is given by $\max_{\varphi} \min_{\psi} \mathfrak{H}$, namely

$$\begin{aligned} \frac{\partial \mathfrak{H}}{\partial \varphi} &= -\lambda_{r_E} \sin \varphi - \frac{\lambda_{\theta} \cos \varphi}{r_E} = 0 \\ \Rightarrow \tan \varphi^* &= -\frac{\lambda_{\theta}}{\lambda_{r_E} r_E} \end{aligned} \quad (6)$$

$$\begin{aligned}\frac{\partial \mathcal{H}}{\partial \psi} &= -\lambda_{r_o} \alpha \sin \psi + \frac{\lambda_\theta \alpha \cos \psi}{r_o} = 0 \\ \Rightarrow \tan \psi^* &= \frac{\lambda_\theta}{\lambda_{r_o} r_o}\end{aligned}\tag{7}$$

The second-order sufficiency condition for φ is

$$\therefore \frac{\partial^2 \mathcal{H}}{\partial \varphi^2} = -\lambda_{r_E} \cos \varphi + \frac{\lambda_\theta \sin \varphi}{r_E} < 0$$

and inserting the expression for φ^* from (6) yields

$$\begin{aligned}\lambda_\theta + \frac{(r_E \lambda_{r_E})^2}{\lambda_\theta} &< 0 \\ \Rightarrow \lambda_\theta(t) &< 0 \quad \forall 0 \leq t < T\end{aligned}\tag{8}$$

Similarly,

$$\therefore \frac{\partial^2 \mathcal{H}}{\partial \psi^2} = -\lambda_{r_o} \alpha \cos \psi - \frac{\lambda_\theta \alpha \sin \psi}{r_o} > 0$$

and inserting the expression for ψ^* from (7) yields

$$\begin{aligned}\lambda_\theta + \frac{(r_o \lambda_{r_o})^2}{\lambda_\theta} &< 0 \\ \Rightarrow \lambda_\theta(t) &< 0 \quad \forall 0 \leq t < T\end{aligned}\tag{9}$$

The expressions for φ^* and ψ^* given in Equations (6) and (7) can also be used to rewrite the state and co-state equations only in terms of the states and co-states. A standard, albeit nonlinear, Two-Point Boundary Value Problem (TPBVP) is obtained on the interval $t = [0, T]$:

$$\left. \begin{aligned}
\dot{r}_E &= \frac{\lambda_{r_E} r_E}{\sqrt{\lambda_{r_E}^2 r_E^2 + \lambda_\theta^2}}, & r_E(0) &= r_{E_0} \\
\dot{r}_O &= \frac{-\alpha \lambda_{r_O} r_O}{\sqrt{\lambda_{r_O}^2 r_O^2 + \lambda_\theta^2}}, & r_O(0) &= 1 \\
\dot{\theta} &= \frac{\lambda_\theta}{r_E \sqrt{\lambda_{r_E}^2 r_E^2 + \lambda_\theta^2}} - \frac{\alpha \lambda_\theta}{r_O \sqrt{\lambda_{r_O}^2 r_O^2 + \lambda_\theta^2}}, & \theta(0) &= \theta_0 \\
\dot{\lambda}_{r_E} &= 4r_E - 2r_O \cos \theta + \frac{\lambda_\theta^2}{r_E^2 \sqrt{\lambda_{r_E}^2 r_E^2 + \lambda_\theta^2}}, & \lambda_{r_E}(T) &= 0 \\
\dot{\lambda}_{r_O} &= 2r_O - 2r_E \cos \theta - \frac{\alpha \lambda_\theta^2}{r_O^2 \sqrt{\lambda_{r_O}^2 r_O^2 + \lambda_\theta^2}}, & \lambda_{r_O}(T) &= 0 \\
\dot{\lambda}_\theta &= 2r_E r_O \sin \theta, & \lambda_\theta(T) &= 0, \quad 0 \leq t \leq T
\end{aligned} \right\} \quad (10)$$

3.2 Suboptimal Approaches

Suboptimal solutions are useful in their own right and provide insight into the differential game. Suboptimal solutions can also be used to provide the first guess for solving the TPBVP (10) of the optimal control/differential game.

3.2.1 Geometric Approach

Using a geometric approach provides a suboptimal but easily implementable solution of the differential game. This approach is suboptimal because the Relay and the Rover each momentarily assume that the other player is stationary when determining their optimal control.

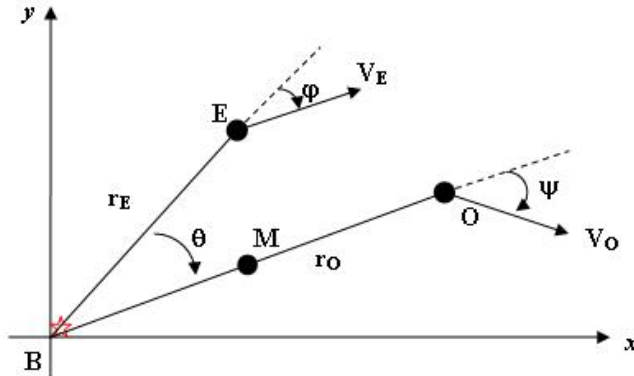


Figure 2: Schematic of Relay System Showing the Midpoint

The geometry of the engagement forms a triangle with vertices E , B and O representing the respective locations of the Relay, Base and Rover (see Figure 2). Let M be the midpoint between the Rover and the Base. Simply rotating the schematic in Figure 2 provides an equivalent schematic (see Figure 3) which is similar to the one analyzed in Appendix A.

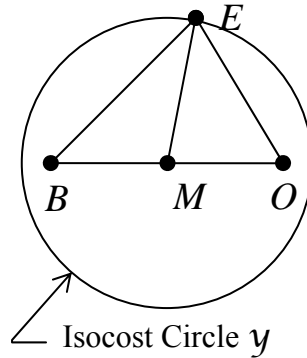


Figure 3: Schematic of Relay System Showing Isocost Circle

If the Rover were stationary, the loci of constant instantaneous costs

$$\gamma = \overline{EO}^2 + \overline{BE}^2$$

for the Relay are concentric circles centered at the midpoint and the midpoint is the Relay location which minimizes the cost (Gutenmacher and Vasilyev, 2004). The Relay is on the circumference of said circles, and the instantaneous cost γ is determined by the position of the Relay. This means that the gradient vector for minimizing cost is in the radial direction. Therefore, the optimal strategy of the Relay is to head toward the midpoint M .

The optimal control of the Relay is determined using the triangle $\triangle ABEM$. The distance between E and M is determined using the law of cosines (just as in determining the distance between E and O before). The control angle φ is then found indirectly by finding its supplementary angle using the law of sines. However, due to an inherent

ambiguity in the law of sines, the control law is specified for three cases: (1) φ is acute, (2) φ is 90° and (3) φ is obtuse.

$$\varphi^* = \begin{cases} \sin^{-1}\left(\frac{r_o \sin \theta}{\sqrt{4r_E^2 + r_o^2 - 4r_E r_o \cos \theta}}\right) & \text{for } r_E < \frac{r_o \cos \theta}{2} \\ \frac{\pi}{2} & \text{for } r_E = \frac{r_o \cos \theta}{2} \\ \pi - \sin^{-1}\left(\frac{r_o \sin \theta}{\sqrt{4r_E^2 + r_o^2 - 4r_E r_o \cos \theta}}\right) & \text{for } r_E > \frac{r_o \cos \theta}{2} \end{cases} \quad (11)$$

This ambiguity can be bypassed by using an inverse cosine function in place of the inverse sine. Thus, the Relay's strategy is:

$$\varphi^* = \cos^{-1}\left(\frac{r_o \cos \theta - 2r_E}{\sqrt{4r_E^2 + r_o^2 - 4r_E r_o \cos \theta}}\right) \quad (12)$$

As far as the Rover is concerned for a worst-case scenario: The Rover is striving to maximize the cost \mathcal{y} at each time instant, assuming that the Relay is stationary. This is accomplished by expanding the isocost circle. The most effective way to expand the isocost circle is to increase the radius \overline{EM} of the circle. When the Relay is stationary, the Rover exclusively controls the position of the midpoint M . The velocity of the midpoint M is always $\frac{1}{2}V_o$, where V_o is the velocity of the Rover, and is always aligned parallel to the velocity vector of the Rover because M is determined by O , and their motion forms two similar triangles (see Figure 4).

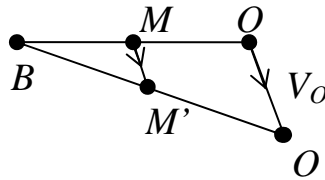


Figure 4: Motion of M and O Forms Similar Triangles

The Rover would like to head in such a direction as to cause the midpoint M to move such that the radius of the isocost circle increases as fast as possible. Hence, to achieve this result, the Rover, which controls the direction of the velocity vector V_O , aligns this vector with the line \overline{EM} , that is, it heads along a path parallel to the Relay. Thus, the Rover's strategy is:

$$\psi^* = \varphi^* - \theta \quad (13)$$

Note that these Relay and Rover strategies are independent of the planning horizon T .

3.2.2 One-Sided Optimization

The complexity of the dynamic optimization problem is significantly reduced by holding one of the MAVs at a fixed position: We will optimize the control of the Relay when the Rover is stationary, that is, $r_O \equiv 1$. The dynamics are the same as previously developed, but now the parameter $\alpha = 0$ and the state space is reduced to $\mathbb{R}^1 \times \mathbb{S}^1$. The optimal control problem is considered:

$$\left. \begin{aligned} \min_{\varphi} \mathcal{Y} &= \int_0^T (2r_E^2 + 1 - 2r_E \cos \theta) dt \\ s.t. & \\ \dot{r}_E &= \cos \varphi, \quad r_E(0) = r_{E_0} \\ \dot{\theta} &= -\frac{1}{r_E} \sin \varphi, \quad \theta(0) = \theta_0, \quad 0 \leq t \leq T \end{aligned} \right\} \quad (14)$$

The new Hamiltonian is

$$\mathfrak{H} = -2r_E^2 - 1 + 2r_E \cos \theta + \lambda_{r_E} \cos \varphi - \lambda_{\theta} \frac{1}{r_E} \sin \varphi \quad (15)$$

According to the Pontryagin Maximum Principle (Pontryagin et al., 1962), the differential equations for the co-states are

$$\left. \begin{aligned} \dot{\lambda}_{r_E} &= 4r_E - 2\cos\theta - \frac{\lambda_\theta \sin\varphi}{r_E^2}, \quad \lambda_{r_E}(T) = 0 \\ \dot{\lambda}_\theta &= 2r_E \sin\theta, \quad \lambda_\theta(T) = 0 \end{aligned} \right\} \quad (16)$$

and the optimality condition is given by $\max_{\varphi} \mathcal{H}$, namely

$$\begin{aligned} \frac{\partial \mathcal{H}}{\partial \varphi} &= -\lambda_{r_E} \sin\varphi - \frac{\lambda_\theta \cos\varphi}{r_E} = 0 \\ \Rightarrow \tan\varphi &= -\frac{\lambda_\theta}{\lambda_{r_E} r_E} \end{aligned} \quad (17)$$

The second-order sufficiency condition is:

$$\therefore \frac{\partial^2 \mathcal{H}}{\partial \varphi^2} = -\lambda_{r_E} \cos\varphi + \frac{\lambda_\theta \sin\varphi}{r_E} < 0 \quad (18)$$

The expression for φ given in Equation (17) is used to rewrite the state and co-state equations only in terms of the states and co-states, obtaining the nonlinear TPBVP

$$\left. \begin{aligned} \dot{r}_E &= \frac{\lambda_{r_E} r_E}{\sqrt{\lambda_{r_E}^2 r_E^2 + \lambda_\theta^2}}, \quad r_E(0) = r_{E_0} \\ \dot{\theta} &= \frac{\lambda_\theta}{r_E \sqrt{\lambda_{r_E}^2 r_E^2 + \lambda_\theta^2}}, \quad \theta(0) = \theta_0 \\ \dot{\lambda}_{r_E} &= 4r_E - 2\cos\theta + \frac{\lambda_\theta^2}{r_E^2 \sqrt{\lambda_{r_E}^2 r_E^2 + \lambda_\theta^2}}, \quad \lambda_{r_E}(T) = 0 \\ \dot{\lambda}_\theta &= 2r_E \sin\theta, \quad \lambda_\theta(T) = 0, \quad 0 \leq t \leq T \end{aligned} \right\} \quad (19)$$

This one-sided optimization problem is easier to solve than the min-max problem initially posed and can therefore be analyzed using typical optimization programs.

GPOCS is a Matlab-based optimization program that uses the ‘‘Gauss pseudospectral method where orthogonal collocation is performed at the Legendre-Gauss points’’ (Tomlab Optimization Inc., 2008) to find the minimizing path of the Relay in this situation.

Appendix B also provides an analysis of the case where the Rover is stationary, but only finds the optimal location of the Relay, not the controls which will guide the Relay to that location (a static optimization approach).

An additional one-sided optimization problem, not considered herein, is obtained when the Rover's point of view is taken, namely, the Relay is stationary and the Rover works to maximize the cost functional.

$$y = \int_0^T (2r_E^2 + r_o^2 - 2r_E r_o \cos \theta) dt$$

3.2.3 Suboptimal Solution Applied to TPBVP

If the geometric approach proves to be an accurate heuristic method, then the initial controls that coordinate with a given initial state can be found using the results from the geometric approach. These initial controls are used with Equations (6) and (7) to find a relationship between the initial co-states. This relationship reduces the number of unknown initial co-states to one, namely, λ_θ .

Choosing an appropriate value for λ_θ will provide the two other initial co-state values needed to solve the nonlinear TPBVP given in Equation (10). Using the values as initial guesses, the optimal initial values of the co-states are found using an iterative method, referred to as a "shooting" method. The process for the shooting method is given below.

1. At the iteration step k , the proposed initial co-states ($\lambda(0) = \lambda_k(0)$) are used with the known initial states ($x(0) = x_k(0)$) to obtain a time history of the nonlinear differential system (10) on the interval $0 \leq t \leq T$ using *ode45* in Matlab. This time history will be referred to as $x_k(t)$ and $\lambda_k(t)$. The final value of the co-states in the history is $\lambda_k(T)$.
2. The differential system is then linearized about the trajectory $x_k(t)$, $\lambda_k(t)$, $0 \leq t \leq T$ to obtain a time-dependent linear system in the perturbations $\delta x_k(t)$, $\delta \lambda_k(t)$:

$$\frac{d}{dt} \begin{pmatrix} \delta x \\ \delta \lambda \end{pmatrix} = A_k(t) \begin{pmatrix} \delta x \\ \delta \lambda \end{pmatrix}, \quad \delta x(0) = 0, \quad \delta \lambda(0) = \delta \lambda_k, \quad 0 \leq t \leq T \quad (20)$$

The A_k matrix is found using the Jacobian function on the differential equations of the system with reference to the states and co-states. Then the values of the states and co-states are substituted into the A_k matrix, resulting in a unique A_k matrix at each time step.

- Then, each of the states and co-states are give an initial unit perturbation which is then propagated using the linear differential system to find the resultant change in states and co-states at $t = T$. This collection of resultant changes is combined to form a resolvent Φ matrix which relates an initial perturbation to a resultant change in state.

$$\begin{pmatrix} \delta x(T) \\ \delta \lambda(T) \end{pmatrix} = \Phi(T) \begin{pmatrix} 0 \\ \delta \lambda_k \end{pmatrix} \quad (21)$$

The Φ matrix can actually be divided into four sub-matrices:

$$\begin{aligned} \Phi &= \begin{bmatrix} \Phi_{1,1} & \Phi_{1,2} \\ \Phi_{2,1} & \Phi_{2,2} \end{bmatrix} \\ \Rightarrow \delta \lambda(T) &= \Phi_{2,2}(T) \delta \lambda_k \end{aligned} \quad (22)$$

- The optimality problem (10) requires that all co-states have a final value equal to zero. Therefore, the goal is for any nonzero final co-states found in step 1 ($\lambda_k(T)$) to be countered by the resultant change in co-state found in step 3 ($\delta \lambda(T)$).

$$\begin{aligned} 0 &= \lambda_k(T) + \delta \lambda(T) \\ &= \lambda_k(T) + \Phi_{2,2}(T) \delta \lambda_k \\ \Rightarrow \delta \lambda_k &= -\Phi_{2,2}^{-1}(T) \lambda_k(T) \end{aligned} \quad (23)$$

Then, by adding the perturbation found in (23), the proposed co-states for the next iteration should result in a final co-state value of zero.

$$\begin{aligned} \lambda_{k+1} &:= \lambda_k + \delta \lambda_k \\ \Rightarrow \lambda_{k+1} &= \lambda_k - \Phi_{2,2}^{-1}(T) \lambda_k(T) \end{aligned} \quad (24)$$

The steps in this shooting method are then repeated until the final co-states $\lambda_k(T)$ converge to zero. It should also be noted that if the sub-matrix $\Phi_{2,2}(1)$ is not invertible, then the generalized inverse of $\Phi_{2,2}(1)$ should be used:

$$\delta \lambda_k = -\Phi_{2,2}^\dagger(T) \lambda_k(T)$$

Specifically, calculate the full rank factorization of $\Phi_{2,2}(1)$.

$$\begin{aligned} \Phi_{2,2}(T) &= HK \\ \Rightarrow \Phi_{2,2}^\dagger(T) &= K^T (KK^T)^{-1} (H^T H)^{-1} H^T \end{aligned}$$

The shooting method yields initial co-states which do not equal zero at the end of the planning horizon, T . Therefore, the co-states are used as initial guesses for another shooting method program. This program uses *ode45* to solve the system of equations (10) for the same time interval ($0 \leq t \leq T$) and iteratively guesses initial conditions for the co-states, using *lsqnonlin*, to minimize the error of the terminal conditions of the co-states, namely, the co-states must equal zero at T .

This final shooting method provides the initial co-states which most closely result in satisfaction of the terminal constraints. However, the performance of the program requires a very good initial guess. The first shooting method provides this initial guess. The flow chart shown in Figure 5 provides a visualization to assist in understanding how the results from the geometric approach are used by the aforementioned Matlab programs to attain full system results. The flow represented here is implemented by a single Matlab program: “*geometry_applied_rdg.m*”.

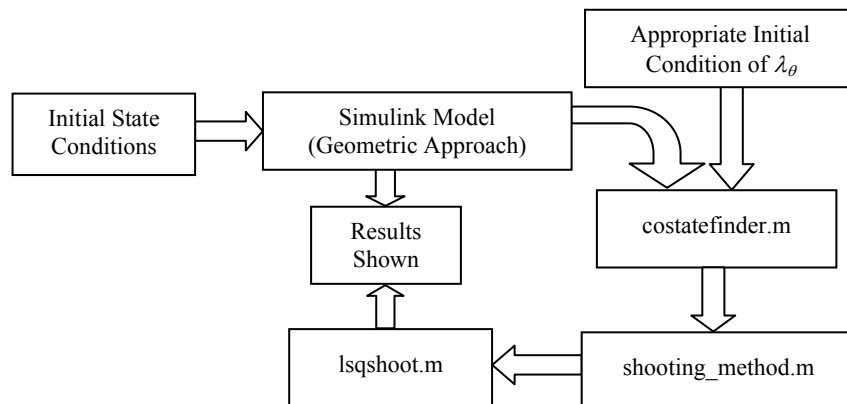


Figure 5: Flow Chart of Matlab Programs Which Produce Full System Results

3.3 Planning Horizon

The Rover uses the services of the Relay as long as $\overline{OE} < \overline{OB}$, for if $\overline{OE} > \overline{OB}$, communication with the Base through the Relay will be counterproductive. In the case

where $\overline{OE} = \overline{OB}$, the geometry of the engagement will form an isosceles triangle and the Rover will lie on the orthogonal bisector of \overline{BE} shown by the dashed line in Figure 6.

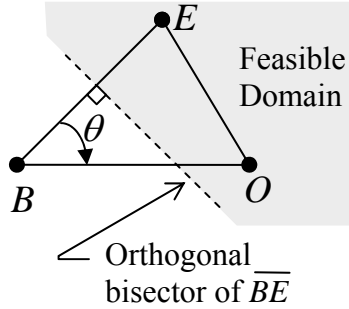


Figure 6: Schematic of Initial Condition Border Line

Therefore, in order to make proper use of the Relay, the state must satisfy the condition

$$0 \leq \theta < \cos^{-1}\left(\frac{1}{2} \frac{r_E}{r_O}\right) \quad (25)$$

The optimal solution of the system will make sense for planning horizons T , provided that the state satisfies Equation (25) $\forall 0 \leq t \leq T$. The geometric considerations-based suboptimal strategies in Figure 7 show that eventually, the orthogonal bisector of the segment \overline{BE} will be crossed by the Rover and hence there must be a maximum planning horizon, depending on the initial values for r_E , r_O and θ . Once the Rover reaches the bisector of the segment \overline{BE} , the game is over.

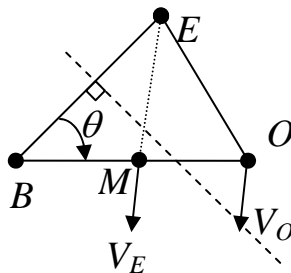


Figure 7: Initial Condition with Limited Planning Horizon

However, if the initial state is as shown in Figure 8, then the maximum possible planning horizon may theoretically approach infinity. That is, condition (25) will not limit the maximum planning horizon; in practice, the planning horizon may still be limited by other factors. For this to be the case, the state must satisfy the condition

$$\theta < \cos^{-1}\left(2\frac{r_E}{r_o}\right) \quad (26)$$

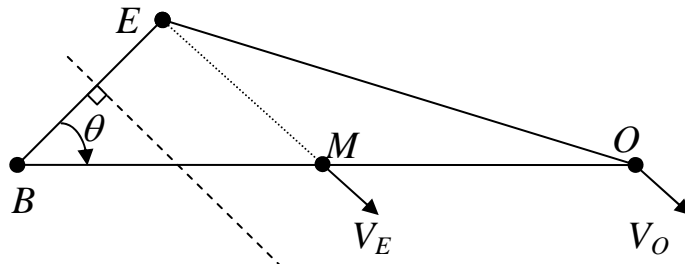


Figure 8: Initial Condition with Unlimited Planning Horizon

Therefore, the maximum possible planning horizon is unbounded by the relation between \overline{OE} and \overline{OB} when

$$0 < \theta < \cos^{-1}\left(2\frac{r_E}{r_o}\right)$$

and is bounded when

$$\cos^{-1}\left(2\frac{r_E}{r_o}\right) < \theta < \cos^{-1}\left(\frac{1}{2}\frac{r_E}{r_o}\right)$$

The maximum planning horizon may also be bounded by the nature of the cost functional: The instantaneous cost

$$y = \overline{EO}^2 + \overline{BE}^2$$

will only depend on \overline{BE} when using the suboptimal geometric considerations-based strategies for the Relay and Rover because \overline{EO} will remain constant for $\alpha = 1$ and does not depend on T . The planning horizon used will allow \overline{BE} to decrease as the Relay moves along the line \overline{EM} until $\overline{BE} \perp \overline{EM}$ at the point E_c , as shown in Figure 9. Once this point is reached, lengthening the planning horizon provides no benefit for the Relay.

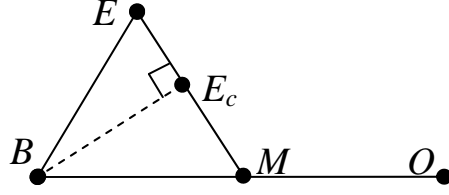


Figure 9: Schematic of Relay Location Closest to Base

This strongly indicates that a conjugate time (T_c) might exist, which would induce an upper bound on the planning horizon. As a first approximation,

$$T_c = \frac{\overline{EE_c}}{V_E} \quad (27)$$

The distance $\overline{EE_c}$ is found by first considering the area of the triangle $\triangle BEM$.

$$S = \frac{1}{4} r_O r_E \sin \theta \quad (28)$$

At the same time,

$$\begin{aligned} S &= \frac{1}{2} \overline{BE_c} \cdot \overline{EM} \\ &= \frac{1}{2} \sqrt{r_E^2 + \frac{1}{4} r_O^2 - r_E r_O \cos \theta} \cdot \overline{BE_c} \end{aligned} \quad (29)$$

Combining Equations (28) and (29) yields

$$\overline{BE_c} = \frac{1}{2} \frac{r_E r_O \sin \theta}{\sqrt{r_E^2 + \frac{1}{4} r_O^2 - r_E r_O \cos \theta}} \quad (30)$$

Finally, $\overline{EE_c}$ is found using the Pythagoras Theorem:

$$\begin{aligned} \overline{EE_c} &= \sqrt{r_E^2 - \overline{BE_c}^2} \\ &= \left[r_E^2 - \frac{r_E^2 r_O^2 \sin^2 \theta}{4r_E^2 + r_O^2 - 4r_E r_O \cos \theta} \right]^{\frac{1}{2}} \\ \Rightarrow \\ \overline{EE_c} &= r_E \left[\frac{4r_E^2 - 4r_E r_O \cos \theta + r_O^2 \cos^2 \theta}{4r_E^2 - 4r_E r_O \cos \theta + r_O^2} \right]^{\frac{1}{2}} \end{aligned} \quad (31)$$

Therefore, the approximate conjugate time is found by inserting Equation (31) into Equation (27)

$$T_c = \frac{r_E}{V_E} \left[\frac{4r_E^2 - 4r_E r_O \cos \theta + r_O^2 \cos^2 \theta}{4r_E^2 - 4r_E r_O \cos \theta + r_O^2} \right]^{\frac{1}{2}} \quad (32)$$

and will require $T < T_c$.

4 Demonstration Hardware and Testing

4.1 Demonstration Configuration

The hardware for the demonstration was provided by the AFIT Advanced Navigation Technology (ANT) Center's laboratory. The hardware presented here will not be used for final production of the ISR and engagement system. It only serves to test and demonstrate the discussed concepts.

4.1.1 Unmanned Aircraft

One of the standard aircraft flown by the ANT Lab is the SIG Manufacturing Company Rascal 110. This aircraft has very stable flight characteristics and a large payload capacity. It has a braced high-wing configuration with a wingspan of 110 inches and a tail wheel. The initial flight testing of the Rascal for the ANT Lab was performed by Jodeh in 2006. The resulting performance, stability and static data were also presented by Jodeh (Jodeh, 2006).



Figure 10: Sig Rascal 110 (©2008 Tower Hobbies)

4.1.2 Autopilot

The autopilot chosen for this demonstration is the Kestrel Autopilot System v 2.2 produced by Procerus Technologies. The autopilot is very compact and weighs only 16.7 grams, making it “the smallest and lightest full featured autopilot on the market” (Procerus, 2008). This autopilot was chosen because it will be able to fit in any aircraft

chosen for the final ISR and engagement system. It was also chosen because Procerus Technologies also offers high quality compatible software (OnPoint Targeting) for video analysis and target recognition. The autopilot is controlled through the included Virtual Cockpit program. This program easily accepts latitude and longitude coordinates to set waypoints for direct flight.



Figure 11: Kestrel Autopilot System (©2008 Procerus Technologies)

4.1.3 Communications Transmission

The standard radio frequency modem used by Procerus for the Kestrel autopilot is the Xtend OEF RF module available from Digi International (formerly MaxStream). These modems operate in the 900 MHz frequency band and have an output power of one watt. The outdoor line-of-sight range is up to 40 miles (with a high gain antenna) and it supports a repeater network topology (Digi Int., 2008).



Figure 12: Xtend OEF RF Module (©2007 Digi International)

4.1.4 Sensor Data Transmission

The system used to transmit and receive data from the on-board camera is a product of Black Widow AV. This set transmits on one of eight channels in the 2.4 GHz frequency band with an output power of one watt. Each unit in the set can operate on a 12 V battery pack while the receiver also comes with an AC adapter (Black Widow AV, 2008).



Figure 13: Black Widow 1 W Transmitter and Receiver Set (©2007 Black Widow AV)

4.1.5 Relay Configuration

The relay for the sensor data was the only relay available for the proof of concept demonstration. The hardware and software required to test a relay for autopilot and control signals was unavailable. The relay consisted of a Black Widow transmitter and

receiver set, where the output of the receiver was directly fed into the input for the transmitter (by the long blue cord seen in Figure 14, below).



Figure 14: Setup for Sensor Data Relay Demonstration

In this configuration, the transmitter (seen on the left side of Figure 15) rebroadcast the data from the receiver (seen on the right side of Figure 15) on a different channel. The receiver and transmitter were also separated so as to avoid any interference between them.

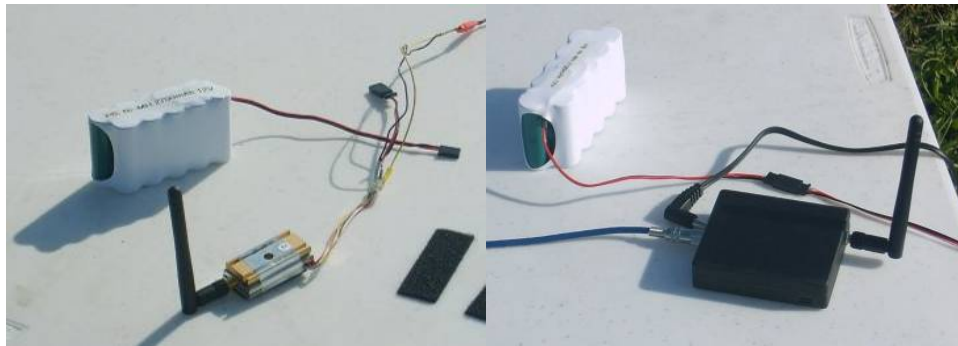


Figure 15: Detail of Setup for Sensor Data Relay Demonstration

4.1.6 Implementation of Relay MAV Guidance

The theoretical analysis showed that the loci of constant instantaneous costs

$$y = \overline{EO}^2 + \overline{BE}^2$$

for the Relay are concentric circles centered at the midpoint of the straight line connecting the Base to the Rover and that this midpoint is the Relay location which minimizes the cost (Gutenmacher and Vasilyev, 2004). Furthermore, the gradient vector

for minimizing the cost is in the radial direction. Therefore, the simplest and most effective way to minimize the instantaneous cost is for the Relay to fly straight to the midpoint.

In the envisioned ISR and engagement system, the controls for both the Rover and the Relay will come from the same ground control unit (GCU). The GCU will also process and record the sensor data from the Rover. In order to reduce the computational demand on the GCU, the implementation of the optimal Relay guidance will only consist of a program which calculates the position of lowest cost at a particular time and then provides this position to the Virtual Cockpit program as a loitering waypoint. This program is called “commrelay.m” (see Appendix C) and is systematically run every few seconds or every time the signal strength drops below a specified threshold. This method does not truly implement the optimal guidance laws derived in the theoretical analysis, but it does guide the Relay to fly straight to the optimal location at a particular time without inhibiting the performance of the rest of the system.

4.2 Testing Procedure

The relay was set up on a six-foot long folding table on top of a berm near the runway. Both the aircraft transmitter and the relay receiver were set to channel one. The relay receiver then output the signal to the relay transmitter, which was set to channel four. The operator at the ground station verified that both channels showed the same data by switching between channel one and channel four. For this test, the receiver and transmitter of the relay were six feet apart, which is one foot shorter than the overall length of the SIG Rascal 110. The test was repeated with the receiver and transmitter of the relay only four feet apart to show a feasible range for smaller aircraft.

5 Results and Analysis

5.1 Numerical Results

The numerical results shown below were all found using Matlab.

5.1.1 Suboptimal Geometric Results

The following numerical results illustrate the evolution of the differential game in the case where $T = 0.25$, $\alpha = 1$, $r_{E_0} = 0.5$, and $\theta_0 = \frac{\pi}{6}$. In the game plane, the Rover always starts from $(x, y) = (1, 0)$. The trajectories show a visualization of the state history, where the Base location is designated by a star at the origin and the final location of each MAV is signified by a triangle. The final midpoint location is designated by a square.

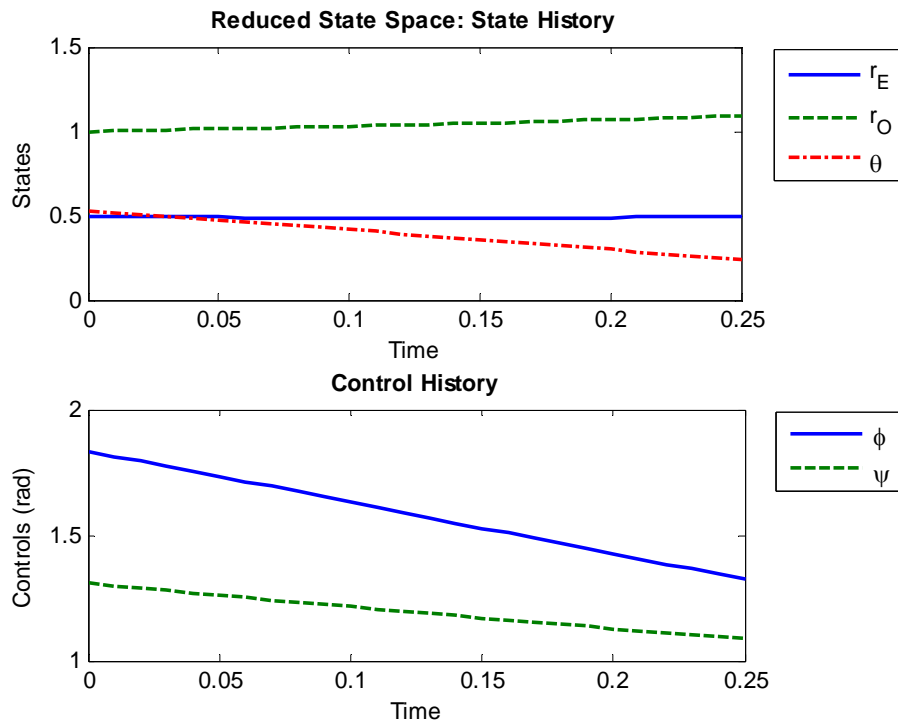


Figure 16: Geometric Time History for $T = 0.25$, $\alpha = 1$, $r_{E_0} = 0.5$, and $\theta_0 = \frac{\pi}{6}$

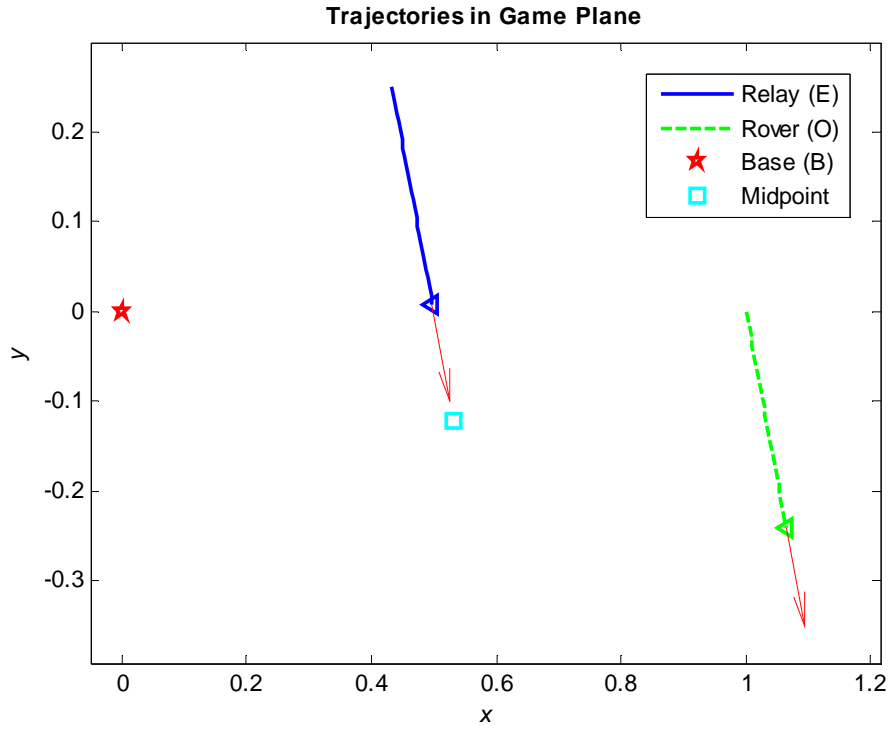


Figure 17: Geometric Spatial Results for $T = 0.25$, $\alpha = 1$, $r_{E_0} = 0.5$, and $\theta_0 = \frac{\pi}{6}$

The following numerical results illustrate the evolution of the differential game in the case where $T = 0.48$, $\alpha = 1$, $r_{E_0} = 0.5$, and $\theta_0 = \frac{\pi}{3}$.

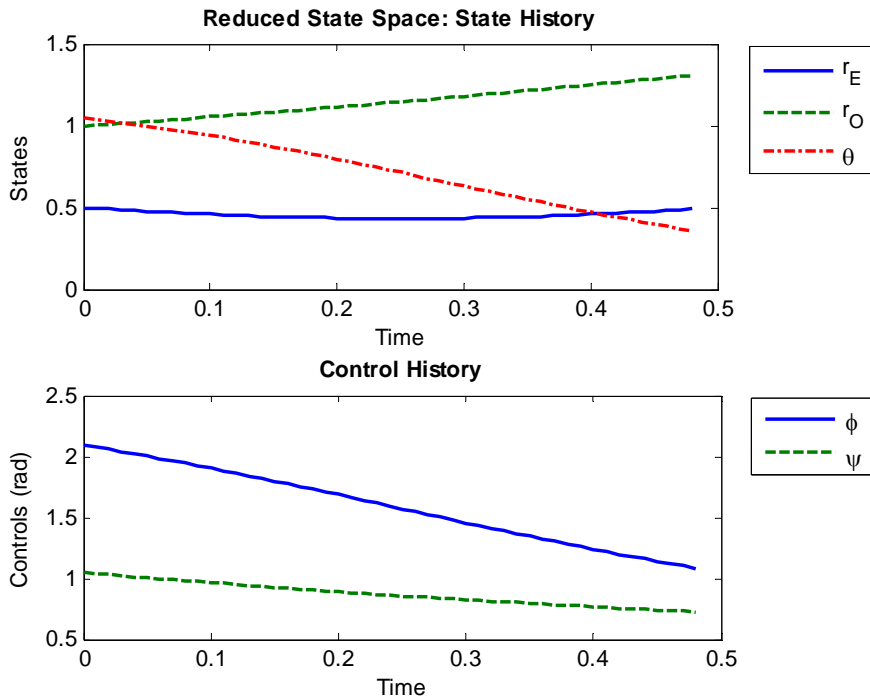


Figure 18: Geometric Time History for $T = 0.48$, $\alpha = 1$, $r_{E_0} = 0.5$, and $\theta_0 = \frac{\pi}{3}$

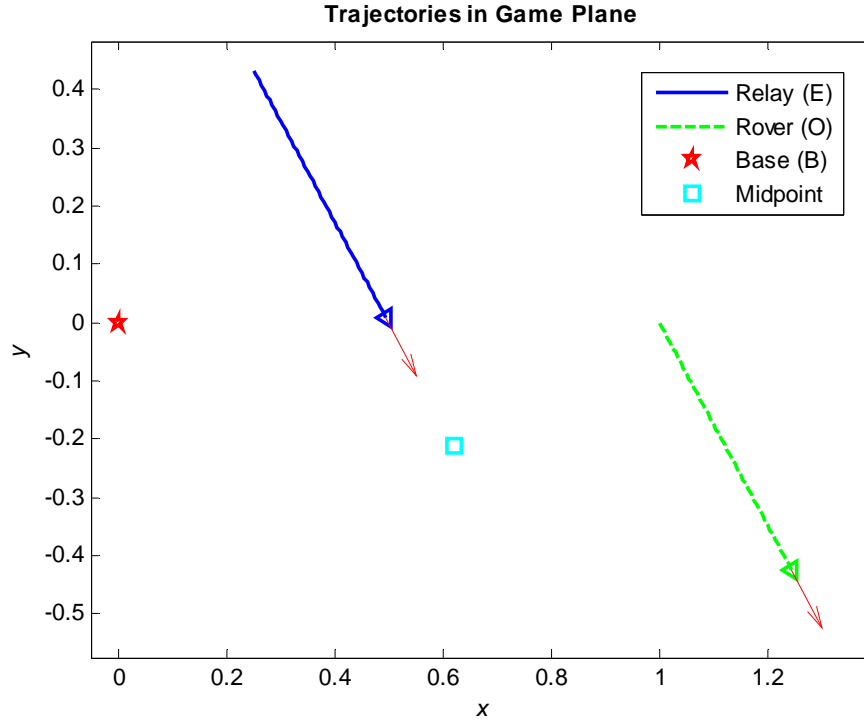


Figure 19: Geometric Spatial Results for $T = 0.48$, $\alpha = 1$, $r_{E_0} = 0.5$, and $\theta_0 = \frac{\pi}{3}$

The results from the scenarios above show that the system performed exactly as designed.

If T is sufficiently large, the three points E , B and O might become collinear.

Once the three points are collinear ($\theta = 0$) the motion is confined to a straight line. The Relay moves toward the midpoint M and the Rover moves away from the Relay. If $\alpha < 2$ the Relay will need to slow down once it reaches the midpoint.

The following numerical results illustrate the evolution of the differential game in the case where $T = 0.5$, $\alpha = 2$, $r_{E_0} = 0.5$, and $\theta_0 = \frac{\pi}{6}$.

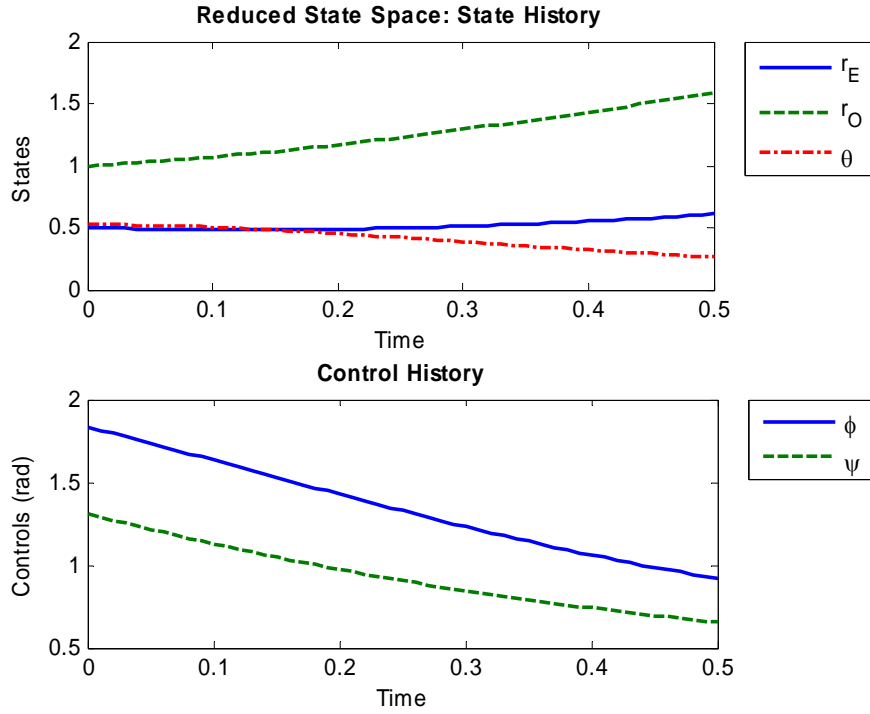


Figure 20: Geometric Time History for $T = 0.5$, $\alpha = 2$, $r_{E_0} = 0.5$, and $\theta_0 = \frac{\pi}{6}$

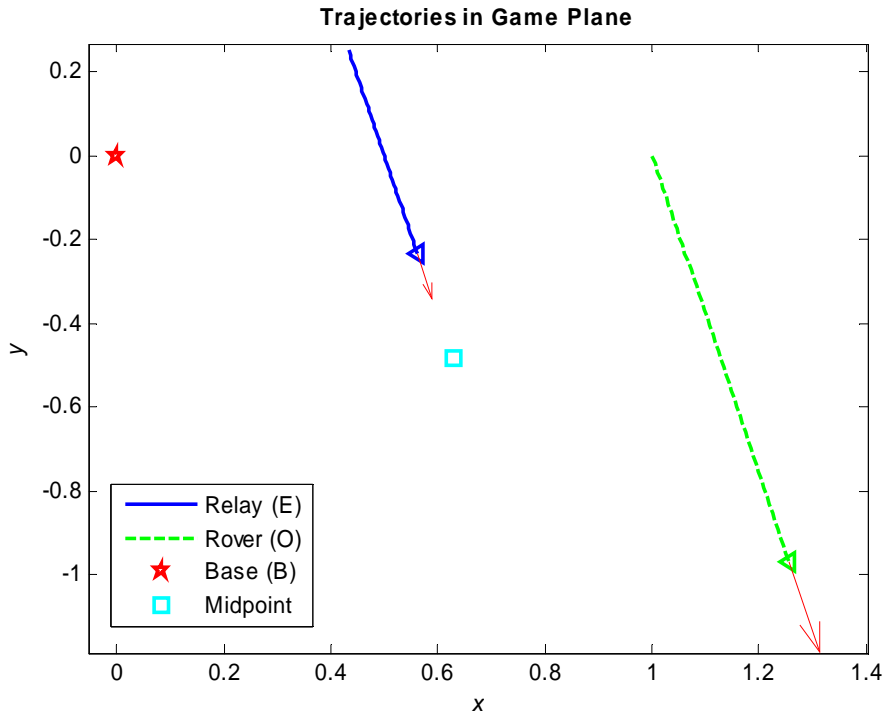


Figure 21: Geometric Spatial Results for $T = 0.5$, $\alpha = 2$, $r_{E_0} = 0.5$, and $\theta_0 = \frac{\pi}{6}$

Once E , B and O are collinear, the reduced Relay velocity eliminates the need for excessive control use. However, it is possible that the Relay might never arrive at the

midpoint due to a short planning horizon T , or the maximizing efforts of the Rover. If the Rover used a suboptimal control strategy (which is common in practice), it is possible for the Relay to arrive at the midpoint and consistently match the motion of the midpoint.

5.1.2 One-Sided Optimization Results

The following numerical results show the solution of the optimization problem for $T = 0.25$, $r_{E_0} = 0.5$, and $\theta_0 = \frac{\pi}{6}$. The co-state initial conditions satisfying the terminal constraints are $\lambda_{r_E}(0) = 0.0347$ and $\lambda_{\theta}(0) = 0.0647$.

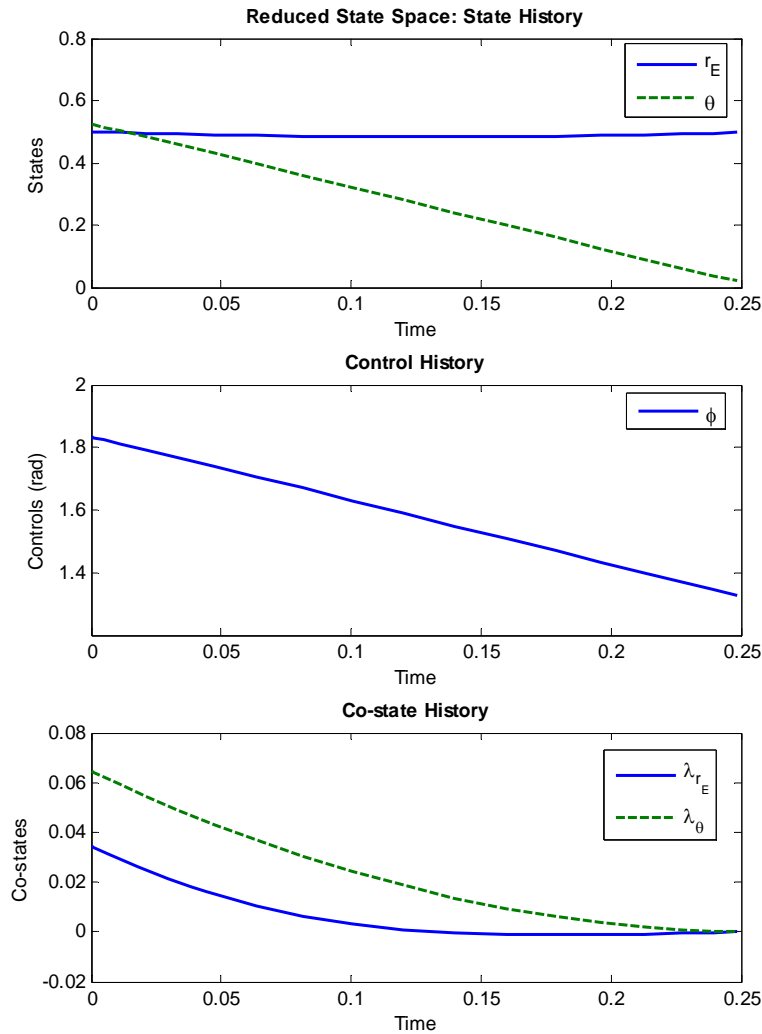


Figure 22: One-Sided Time History for $T = 0.25$, $r_{E_0} = 0.5$, and $\theta_0 = \frac{\pi}{6}$

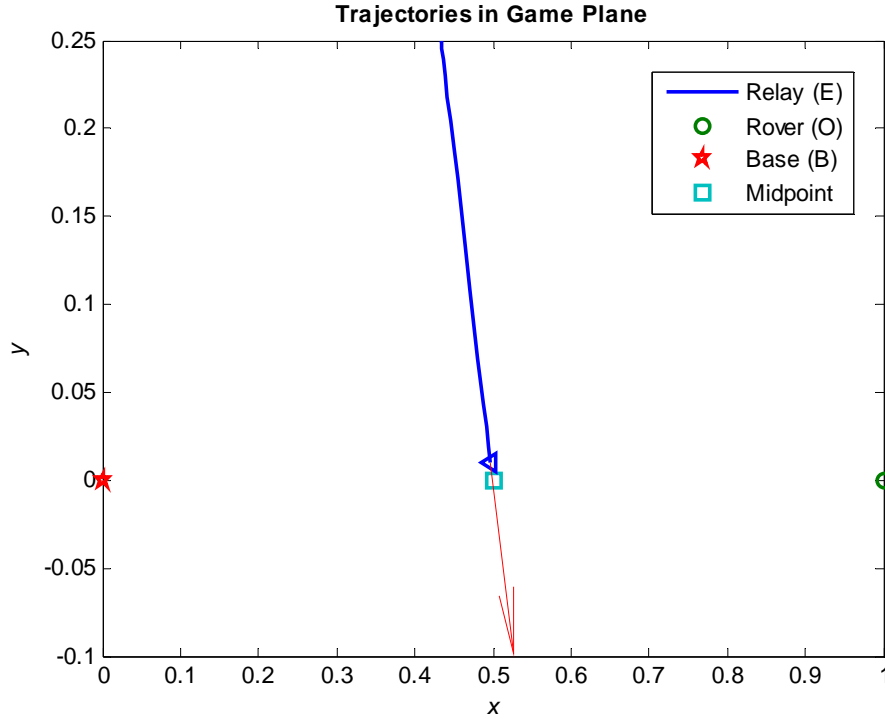


Figure 23: One-Sided Spatial Results for $T = 0.25$, $r_{E_0} = 0.5$, and $\theta_0 = \frac{\pi}{6}$

It is important to note that the slope of the path traveled by the Relay maintains a constant value of 105° (measured counter-clockwise from the x -axis). The slope time history of the path has a numerical standard deviation of 0.0153° . This shows that the Relay travels along the straight-line path toward the midpoint M. This corroborates nicely with the heuristic solution found using the geometric approach.

The following numerical results show the solution of the optimization problem for $T = 0.48$, $r_{E_0} = 0.5$, and $\theta_0 = \frac{\pi}{3}$. The co-state initial conditions satisfying the terminal constraints are $\lambda_{r_E}(0) = 0.25$ and $\lambda_\theta(0) = 0.2165$.

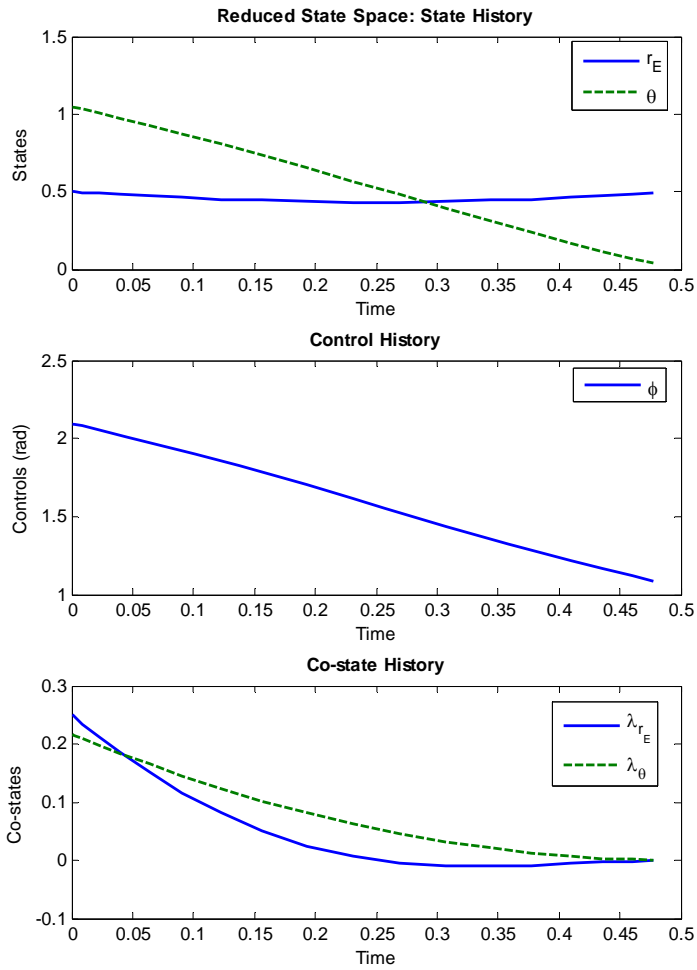


Figure 24: One-Sided Time History for $T = 0.48$, $r_{E_0} = 0.5$, and $\theta_0 = \frac{\pi}{3}$

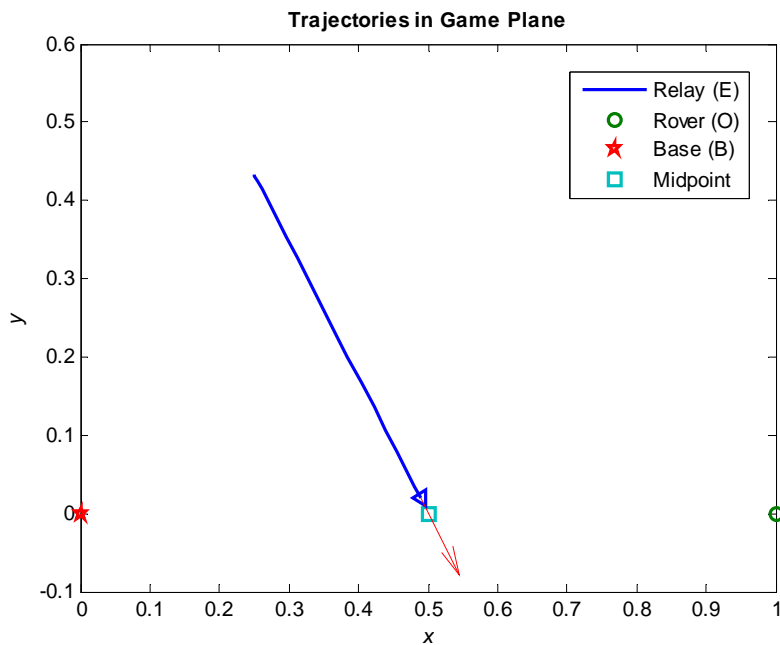


Figure 25: One-Sided Spatial Results for $T = 0.48$, $r_{E_0} = 0.5$, and $\theta_0 = \frac{\pi}{3}$

Similar to the first case, the slope of the path traveled by the Relay maintains a constant value of 120° (measured counter-clockwise from the x -axis). The slope time history of the path has a numerical standard deviation of 0.0193° . This shows that the optimal solution is indeed a straight line path toward the midpoint between the Base and the Rover.

5.1.3 Results Using Complete System

The suboptimal solutions provide corroborating results, showing that the optimal control of the Relay is to fly directly toward the midpoint between the Rover and the Base. The optimal control for the Rover to reverse this action would be to fly parallel to the Relay, as suggested in the suboptimal geometric consideration. Therefore, the nonlinear TPBVP given by Equation (10) is solved using the two shooting methods described previously. These shooting methods find the initial co-states by using the data obtained from the geometric approach with Equations (6) and (7), and an appropriate value for λ_θ . To provide an easier comparison, the game plane results of the geometric approach are repeated with the results found using the shooting methods in the figures below.

The following numerical results show the solution of the differential game where $T = 0.25$, $\alpha = 1$, $r_{E_0} = 0.5$ and $\theta_0 = \frac{\pi}{6}$. The initial co-states which most closely satisfy the terminal constraints are $\lambda_{r_E}(0) = -0.0185$, $\lambda_{r_o}(0) = -0.3126$ and $\lambda_\theta(0) = -0.0838$. The resulting terminal co-states are $\lambda_{r_E}(T) = 0.0$, $\lambda_{r_o}(T) = 0.0018$ and $\lambda_\theta(T) = -0.0001$.

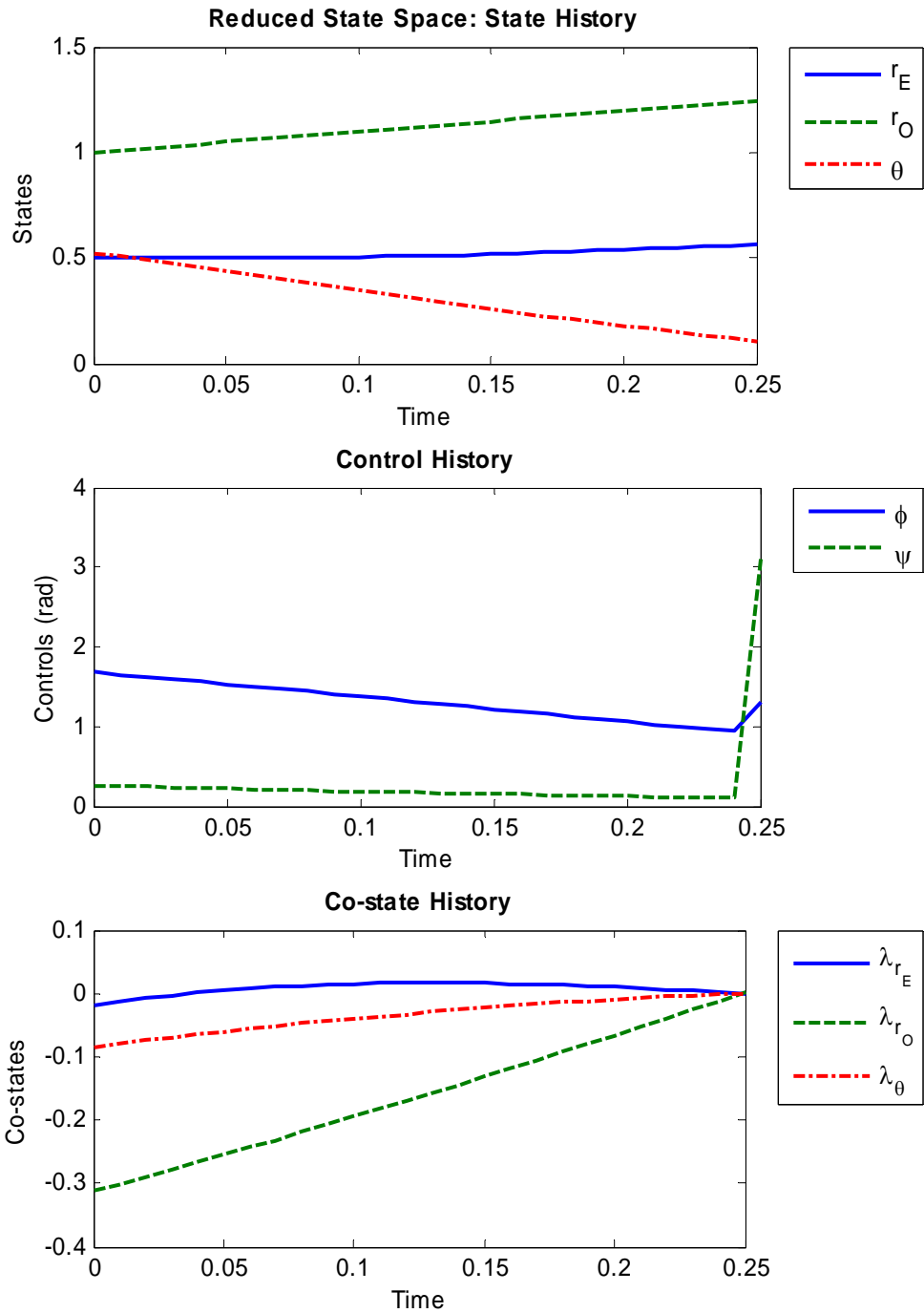


Figure 26: Full System Time History for $T = 0.25$, $\alpha = 1$, $r_{E_0} = 0.5$ and $\theta_0 = \frac{\pi}{6}$

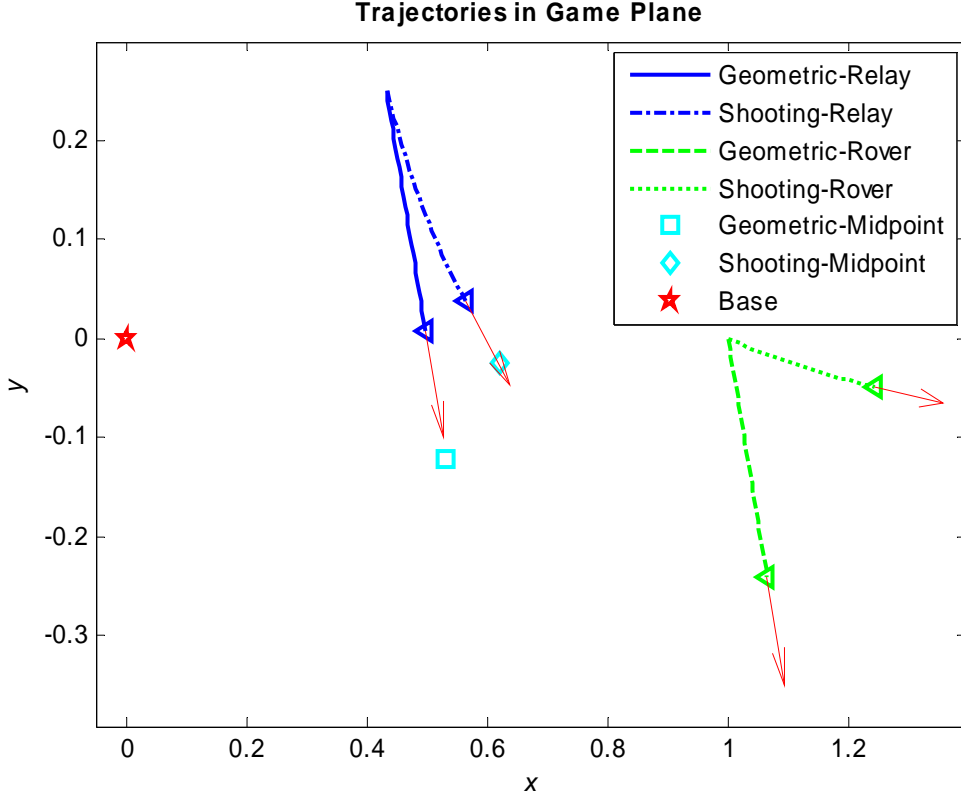


Figure 27: Comparative Spatial Results for $T = 0.25$, $\alpha = 1$, $r_{E_0} = 0.5$ and $\theta_0 = \frac{\pi}{6}$

These results differ from the geometric approach, but the geometric approach is suboptimal. This may be the closest result to an optimal solution to the differential game for the given initial condition, since the second-order sufficiency conditions (given by equations (8) and (9)) are satisfied and the terminal co-states are very near zero. It appears that the Relay is still heading toward M , but the Rover's strategy has changed considerably.

The results in Figures 28 and 29 show the solution of the differential game where $T = 0.48$, $\alpha = 1$, $r_{E_0} = 0.5$ and $\theta_0 = \frac{\pi}{3}$. The initial co-states which most closely satisfy the terminal constraints are $\lambda_{r_E}(0) = -0.4112$, $\lambda_{r_O}(0) = -0.9082$ and $\lambda_\theta(0) = -0.3875$. The resulting terminal co-states are $\lambda_{r_E}(T) = -0.0$, $\lambda_{r_O}(T) = -0.1007$ and $\lambda_\theta(T) = -0.1018$.

These results also differ from the geometric approach. It appears that the Relay is no longer heading toward M , but the terminal co-states also have a greater error from the constraints. The second-order sufficiency conditions (given by equations (8) and (9)) are still satisfied.

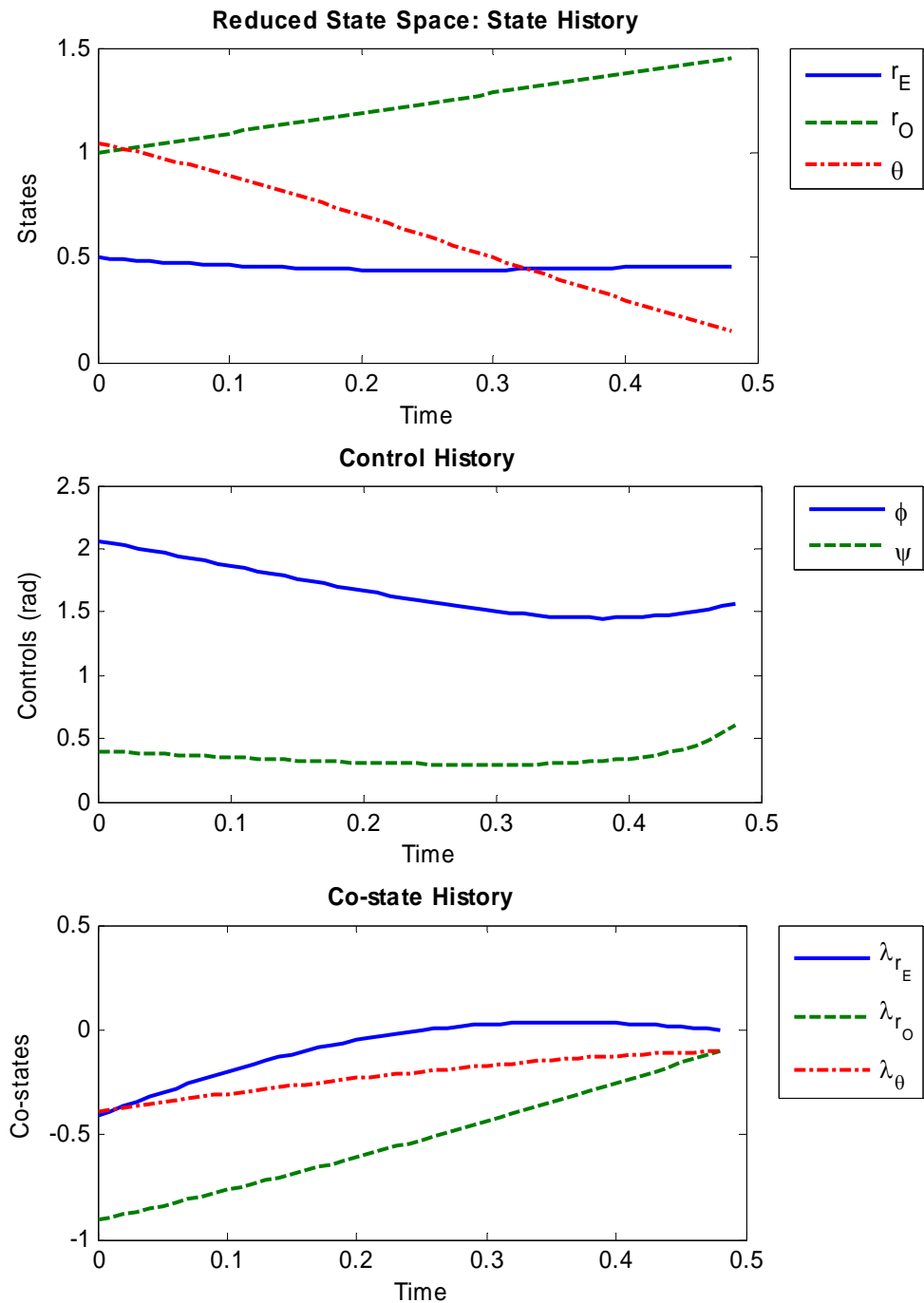


Figure 28: Full System Time History for $T = 0.48$, $\alpha = 1$, $r_{E_0} = 0.5$ and $\theta_0 = \frac{\pi}{3}$

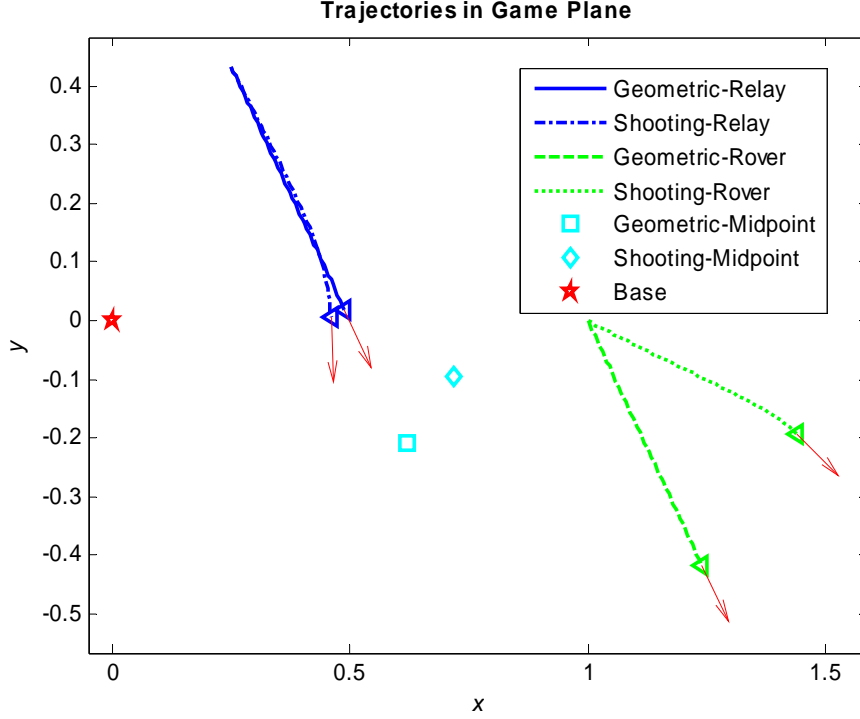


Figure 29: Comparative Spatial Results for $T = 0.48$, $\alpha = 1$, $r_{E_0} = 0.5$ and $\theta_0 = \frac{\pi}{3}$

The results in Figures 30 and 31 show the solution of the differential game where $T = 0.5$, $\alpha = 2$, $r_{E_0} = 0.5$, and $\theta_0 = \frac{\pi}{6}$. The initial co-states which most closely satisfy the terminal constraints are $\lambda_{r_E}(0) = -15.3439$, $\lambda_{r_o}(0) = 1.8354$, and $\lambda_\theta(0) = -0.0628$. The resulting terminal co-states are $\lambda_{r_E}(T) = -0.0$, $\lambda_{r_o}(T) = -0.0141$ and $\lambda_\theta(T) = 0.0209$.

These results were much unexpected. The scenario represents a special case where the Relay moves at the same speed as M ($\alpha = 2$). Therefore, these results are possibly due to unforeseen physics present in the system. The results may also be due to an improper value for the planning horizon, T . The terminal co-states are very near zero but the second-order sufficiency conditions are not satisfied, since λ_θ starts out negative and ends positive. Therefore, it may be possible that this result gives the opposite goal of optimization, namely, the Relay ends up trying to maximize the cost while the Rover tries to minimize the cost. This may also be simply due to the fact that a sixth order, nonlinear

TPBVP is very complex and non-intuitive. Regardless of these conjectures, no observed initial values for λ_θ have provided results which differ from those seen here. This provides more incentive for further research of the system and the nonlinear TPBVP given by Equation (10).

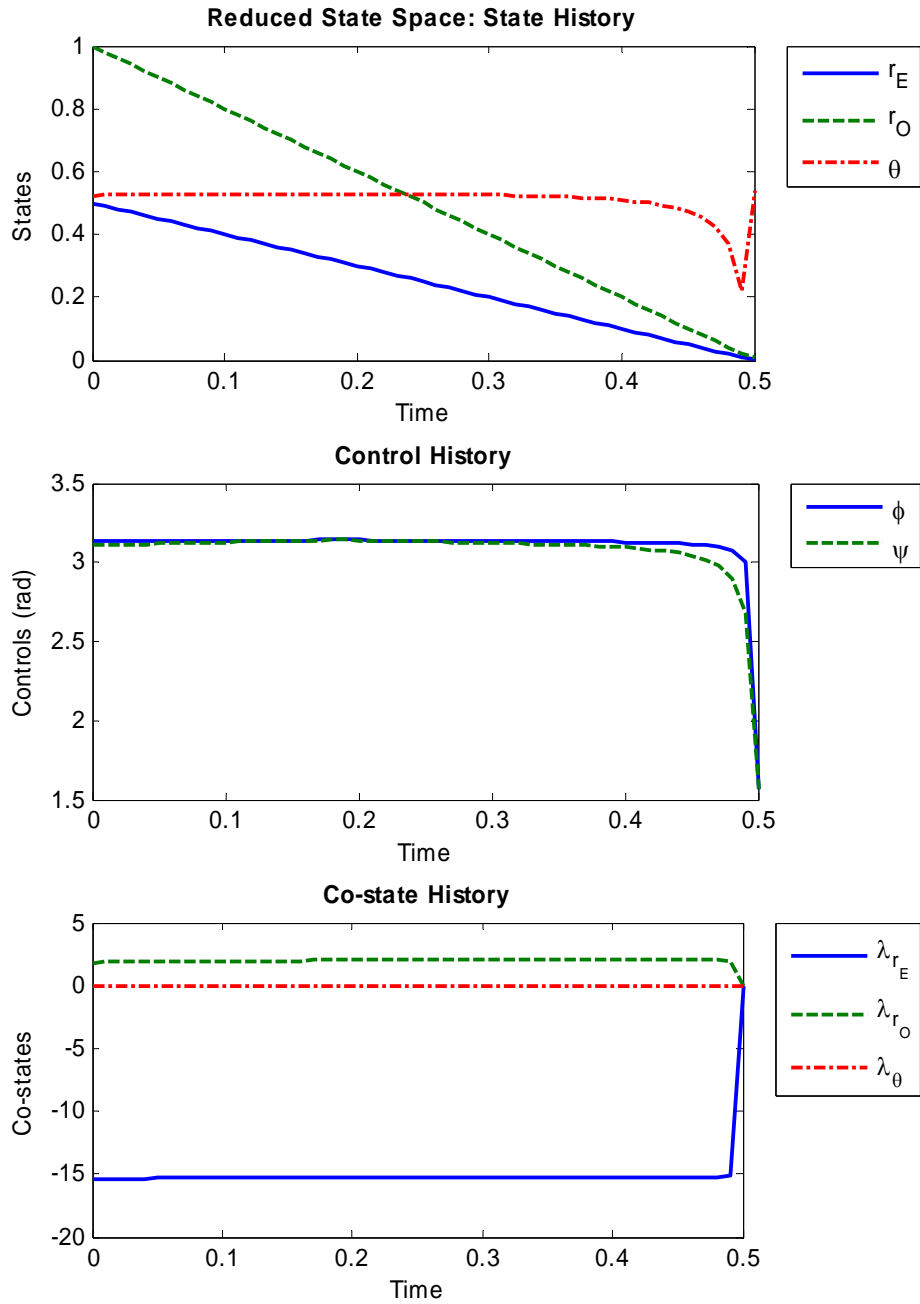


Figure 30: Full System Time History for $T = 0.5$, $\alpha = 2$, $r_{E_0} = 0.5$, and $\theta_0 = \frac{\pi}{6}$

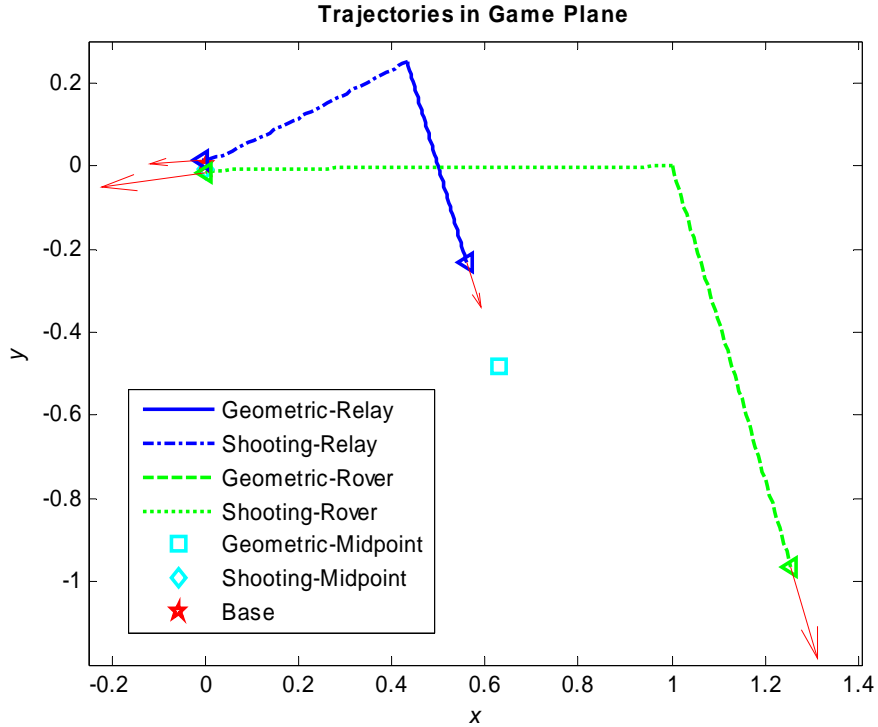


Figure 31: Comparative Spatial Results for $T = 0.5$, $\alpha = 2$, $r_{E_0} = 0.5$, and $\theta_0 = \frac{\pi}{6}$

5.2 Test Results

The concept demonstration for the sensor data relay was performed at Camp Atterbury Army National Guard Base in Indiana on November 9, 2007. During the first test, the rebroadcast signal from the relay had some static but showed the same picture as the original signal being broadcast from the aircraft. This static can be avoided in future applications by using a higher quality receiver for the relay (e.g., a diversity receiver). The test was repeated with the receiver and transmitter of the relay only four feet apart. This change in configuration gave the same results as the first test. Therefore, if the Relay has at least four feet of usable space in the fuselage of the aircraft, interference should not be a main cause of concern.

The practical Implementation of the Relay guidance has been proven using a Hardware-in-the-Loop simulation with the Fleeting Target Controller developed by Sakryd and Ericson in conjunction with this study.

6 Conclusions and Recommendations

6.1 Conclusions

This thesis developed optimal guidance laws for a Relay MAV in support of ISR beyond LOS. The guidance laws are based upon the solution of a min-max optimization problem, namely, the solution of the differential game, which represents a worst case scenario. The solution of the differential game hinges on the solution of a nonlinear TPBVP.

Suboptimal Relay (and Rover) guidance strategies are first provided. The first of these suboptimal guidance strategies is derived using a geometry-based (sub)optimality principle. The Relay heads toward the instantaneous midpoint of the straight line between the Rover and the Base. The Rover, heads away from the Relay on a course parallel to that of the Relay. The second suboptimal guidance strategy is a one-sided Relay optimal control problem, where the Rover is considered stationary. The results using the Matlab optimization program GPOCS showed that the optimal guidance of the Relay is to fly directly toward the instantaneous midpoint of the straight line between the Rover and the Base.

The heuristic methods provided corroborating results which were then used as first guesses for a combination of two shooting methods in series to solve the TPBVP. The shooting method results yielded the approximate numerical solution of the Relay-Rover differential game.

The practical Implementation of the Relay guidance consists of a Matlab program which calculates the Relay position which requires the lowest RF power (i.e., the midpoint between the Rover and the Base) at a particular time and then provides this

position to the Virtual Cockpit program as a loitering waypoint. The program relies on the Kestrel autopilot to fly toward the waypoint and loiter there until it receives a new loitering waypoint. This program has been proven using a Hardware-in-the-Loop simulation with the Fleeting Target Controller. The hardware configuration required to relay sensor data consisted of a ground-based receiver/transmitter set which received the data and fed it directly to the transmitter, which transmit it on a different channel. This configuration was tested and proved that the concept is feasible for future use on an aircraft.

6.2 Recommendations

The following recommendations would help provide more robust and realistic guidance laws for the system.

- Analyze the relationship between the initial states and initial co-states to find a more routine method to find a solution to the TPBVP.
- Use a different method (i.e., different from the “shooting method”) to analyze the complete system.
- Perform another one-sided optimization from the Rover’s point of view (i.e., trying to maximize the cost while the Relay is stationary).
- Use a more realistic system model, which considers wind effects and aircraft attitude.
- Incorporate more realistic constraints on the differential equations of motion (e.g., maximum turn rate, stall speed, etc.).
- Consider the signal strength or signal-to-noise ratio as a driving factor for finding the optimal relay location and guidance laws.
- Analyze the effect of the speed ratio α and determine if there is an optimal value for both arriving at the optimal location and matching its movements.

Appendix A – Geometry

An Elementary Euclidean Geometry Result:

It is well known that the locus of all points such that the sum of the distances from two fixed points is constant, is an ellipse. Thus, the following is of some interest.

Theorem 1 The Locus of all points such that the sum of the squares of the distances from two fixed points is constant, is a circle centered at the midpoint of the segment formed by the two fixed points. The radius of this circle is

$$R = \sqrt{d^2 - f^2}$$

where the sum of the squares of the distances is $2d^2$ and the distance between the fixed points is $2f$, obviously, $d \geq f$.

Proof:

Let the fixed points F_1 and F_2 be on the x -axis ($F_1 = (f, 0)$, $F_2 = (-f, 0)$) as shown in the figure below.

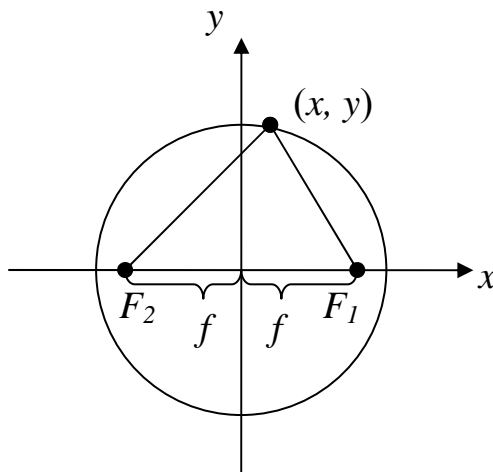


Figure 32: Schematic of Fixed Points Showing Isocost Circle

The sum of the squares of the distances is calculated as

$$\begin{aligned}
2d^2 &= (f+x)^2 + y^2 + (f-x)^2 + y^2 \\
&= 2f^2 + 2x^2 + 2y^2 \\
\Rightarrow x^2 + y^2 &= d^2 - f^2
\end{aligned}$$

This is the equation of a circle centered at the origin, whose radius is

$$R = \sqrt{d^2 - f^2}$$

□

This result appeared in Gutenmacher and Vasilyev (2004).

Remark: The loci of constant costs, $2d^2$, are concentric circles where the minimum cost is found at the midpoint of the line formed by F_1 and F_2 , where $d = f$.

Extension: The Locus of all points such that the weighted sum of the squares of the distances from two fixed points is constant, is a circle centered on the segment formed by the two fixed points and is at a distance of $(1 - 2\alpha)f$ from this segment's midpoint.

The radius of this circle is

$$R = \sqrt{d^2 - 4\alpha(1-\alpha)f^2}$$

where d^2 is the specified weighted sum of the squares of the distances, the distance between the fixed points is $2f$; and the weight is α ; if $\alpha < 0$ or $\alpha > 1$ this is true $\forall d > 0$, and if $0 \leq \alpha \leq 1$, $d > 2f\sqrt{\alpha(1-\alpha)}$. Note: When the weight $\alpha = 1/2$, need $d > f$.

Proof: The weighted sum of the squares of the distances is calculated as

$$\begin{aligned}
d^2 &= \alpha[(f+x)^2 + y^2] + (1-\alpha)[(f-x)^2 + y^2] \\
&= \alpha f^2 + \alpha x^2 + 2\alpha fx + \alpha y^2 + (1-\alpha)f^2 + (1-\alpha)x^2 - 2(1-\alpha)fx + (1-\alpha)y^2 \\
&= f^2 + x^2 + y^2 - 2fx(1-2\alpha) \\
&= [x - (1-2\alpha)f]^2 + f^2 + y^2 - (1-2\alpha)^2 f^2 \\
\Rightarrow [x - (1-2\alpha)f]^2 + y^2 &= d^2 - 4\alpha(1-\alpha)f^2
\end{aligned}$$

□

Appendix B – Static Optimization Approach

Observing the system statically can provide insight on the differential game by providing the optimal placement of the MAVs if their motion were momentarily frozen. This approach will provide the optimal placement of the Relay relative to the Rover location. The goal is to minimize the cost functional given in Equation (1) below, which is the integrand of the original differential game. Therefore, the static optimization problem is

$$\left. \begin{aligned} \min_{r_E, \theta} \mathbf{y}(r_E, \theta) &= 2r_E^2 + r_O^2 - 2r_E r_O \cos \theta \\ \text{s.t.} \\ g_1(r_E, \theta) &= -r_E \leq 0 \\ g_2(r_E, \theta) &= -\pi - \theta \leq 0 \\ g_3(r_E, \theta) &= \theta - \pi \leq 0 \end{aligned} \right\} \quad (1)$$

Transforming the problem into a Lagrange form gives

$$L(r_E, \theta, \lambda, s) = 2r_E^2 + r_O^2 - 2r_E r_O \cos \theta + \nu_1(-r_E + s_1^2) + \nu_2(-\pi - \theta + s_2^2) + \nu_3(\theta - \pi + s_3^2) \quad (2)$$

The first-order KKT necessary conditions for optimality (Karush, 1939; Kuhn and Tucker, 1951) for this function are

$$\left. \begin{aligned} L_{r_E}(r_E, \theta, \nu, s) = 0 &\Rightarrow 4r_E - 2r_O \cos \theta - \nu_1 = 0 \\ L_{\theta}(r_E, \theta, \nu, s) = 0 &\Rightarrow 2r_E r_O \sin \theta - \nu_2 + \nu_3 = 0 \\ L_{\lambda}(r_E, \theta, \nu, s) = 0 &\Rightarrow \begin{bmatrix} -r_E + s_1^2 \\ -\pi - \theta + s_2^2 \\ \theta - \pi + s_3^2 \end{bmatrix} = \begin{bmatrix} 0 \\ 0 \\ 0 \end{bmatrix} \\ L_s(r_E, \theta, \nu, s) = 0 &\Rightarrow \begin{bmatrix} 2s_1\nu_1 \\ 2s_2\nu_2 \\ 2s_3\nu_3 \end{bmatrix} = \begin{bmatrix} 0 \\ 0 \\ 0 \end{bmatrix} \end{aligned} \right\} \quad (3)$$

The set of equations given in (3) can be solved because there are eight unknowns in eight equations. However, the problem will first be solved without constraints to determine if the enforcement of said constraints is necessary. The first two equations in

(3) are solved using *fsolve* in Matlab with the Lagrange multipliers set to zero ($v_i = 0$).

Matlab provides the following output:

```
[ rEopt, thetaopt,    cost]
[ 1/2*r0,          0, 1/2*r0^2]
[          0,    -pi/2,    r0^2]
[          0,     pi/2,    r0^2]
```

Each row of the output represents a stationary point of the system which could provide a maximum or minimum cost. None of these stationary points violate the given constraints so solving the full set of eight equations is unnecessary. The first of the three stationary points is the minimum (as shown by the cost given in the last column).

Therefore, given the Rover's position, the midpoint between the Rover and the Base is the optimal location of the Relay to minimize the integrand for the differential game. This result corroborates with the work done by Goldenberg et al. (2004).

Appendix C – Practical Relay Guidance Code

Commrelay Program

```
function [wpx, wpy]=commrelay(uavx,uavy)
% Communication Relay MAV Positioning
% This function returns the x & y coordinates of the optimal location for a
% Relay MAV given the x&y coordinates (relative to the Base) of the Rover
% MAVs flying the ISR mission. The x&y coordinates returned are best input
% as a waypoint for the autopilot to fly toward/loiter around.
%
% by John Hansen, 05 November 2007
% modified: 10 Dec 07, JH: added robustness for inputs

if nargin==2
    [r,c]=size(uavx);
    if r<c
        uavx=uavx';
        uavy=uavy';
    end
    P=[uavx, uavy]
elseif nargin==0
    disp('WARNING: No inputs received! Proceeding using arbitrary
        location');
    disp('for two MAVs. ');
    P=[20 40;-20 40]
else
    disp('Incorrect number of inputs. Need two inputs: ');
    disp('1: x-values of MAV(s)');
    disp('2: y-values of MAV(s)');
end
%% Initial Guess
x0=[mean(P(:,1))/2+1;mean(P(:,2))/2]-1];
%% Optimization
options = optimset('display','iter','GradObj','off','GradConstr','off', ...
    'DerivativeCheck','off','TolCon', 1e-8, 'TolX', 1e-8);
[x,mincost,ExitFlag,Output]=fminunc(@objective,x0,options,P);
Output
wpx=x(1)
wpy=x(2)
return

%% the cost function%%%%%%%%%%%%%%%%%%%%%%%%%%%%%%%%%%%%%%%%
function [cost]=objective(x,P)
n=length(P(:,1));
f0=n*x(1)^2+n*x(2)^2;
for j=1:n
    f(j)=(x(1)-P(j,1))^2+(x(2)-P(j,2))^2;
end
cost=f0+sum(f);
```

Bibliography

- Basu, P. and Redi, J., "Movement Control Algorithms for Realization of Fault-Tolerant Ad Hoc Robot Networks," *IEEE Network*, Vol. 18, No. 4, July/August 2004, pp. 36, 0890-8044.
- Black Widow AV, "2.4Ghz 1000mW Transmitter and Receiver Set," Retrieved January 28, 2008 from <http://www.blackwidowav.com/bwav2401000components.html>
- Brown, T. X., Argrow, B., Dixon, C., Doshi, S., Thekkekunnel, R.-G., and Henkel, D., "Ad Hoc UAV Ground Network (AUGNET)," In AIAA 3rd "Unmanned Unlimited" Technical Conference, Chicago IL, September 20-23, 2004.
- Digi International, "XTend OEF RF Modules Product Datasheet," Retrieved January 28, 2008 from http://www.digi.com/pdf/ds_xtendmodule.pdf
- Dixon, C. R. and Frew, E. W., "Cooperative Electronic Chaining Using Small Unmanned Aircraft," In *AIAA Infotech@Aerospace*, AIAA, Rohnert Park CA, May 2007.
- Floreano, D., Hauert, S., Leven, S., and Zufferey, J.-C., "Evolutionary Swarms of Flying Robots," In *International Symposium on Flying Insects and Robots*, August 2007, pp. 35-36.
- Goldenberg, D., Lin, J., Morse, A. S., Rosen, B. E., and Yang, Y. R., "Towards Mobility as a Network Control Primitive," In *ACM Mobihoc '04*, Tokyo, 24-26 May 2004.
- Gutenmacher, V., and Vasilyev, N. B., *Lines and Curves*, Birkhäuser Boston, Boston MA, 2004, pp. 23-24.
- Jodeh, Nidal M., *Development of Autonomous Unmanned Aerial Vehicle Research Platform: Modeling, Simulating, and Flight Testing*, MS Thesis, AFIT/GAE/ENY/06-M18, School of Engineering and Management, Air Force Institute of Technology (AU), Wright-Patterson AFB OH, March 2006.
- Karush, W., "Minima of Functions of Several Variables with Inequalities as Side Constraints", M.Sc. Dissertation, Dept. of Mathematics, Univ. of Chicago, 1939.
- Kuhn, H. W. and Tucker, A. W., "Nonlinear Programming", *Proceedings of 2nd Berkeley Symposium*, Berkeley: University of California Press, 1951, pp. 481-492.
- Pontryagin, L. S., Boltyanskii, V. G., Gamkrelidze, R. V., and Mishchenko, E. F., *The Mathematical Theory of Optimal Processes*, John Wiley, New York NY, 1962.
- Procerus Technologies, "Kestrel Autopilot v2.2 Data Sheet," Retrieved January 29, 2008 from http://www.procerusuav.com/Documents/Kestrel_2.2.pdf
- Tomlab Optimization Inc., "GPOCS – Optimal Control Software," Retrieved February 19, 2008 from <http://gpocs.com>

REPORT DOCUMENTATION PAGE

Form Approved
OMB No. 074-0188

The public reporting burden for this collection of information is estimated to average 1 hour per response, including the time for reviewing instructions, searching existing data sources, gathering and maintaining the data needed, and completing and reviewing the collection of information. Send comments regarding this burden estimate or any other aspect of the collection of information, including suggestions for reducing this burden to Department of Defense, Washington Headquarters Services, Directorate for Information Operations and Reports (0704-0188), 1215 Jefferson Davis Highway, Suite 1204, Arlington, VA 22202-4302. Respondents should be aware that notwithstanding any other provision of law, no person shall be subject to a penalty for failing to comply with a collection of information if it does not display a currently valid OMB control number.

PLEASE DO NOT RETURN YOUR FORM TO THE ABOVE ADDRESS.

1. REPORT DATE (DD-MM-YYYY) 27-03-2008		2. REPORT TYPE Master's Thesis		3. DATES COVERED (From - To) Jun 2007 - Mar 2008		
4. TITLE AND SUBTITLE Optimal Guidance of a Relay MAV for ISR Support Beyond Line-of-Sight				5a. CONTRACT NUMBER		
				5b. GRANT NUMBER		
				5c. PROGRAM ELEMENT NUMBER		
6. AUTHOR(S) Hansen, John H., 2d Lt, USAF				5d. PROJECT NUMBER JON 195		
				5e. TASK NUMBER		
				5f. WORK UNIT NUMBER		
7. PERFORMING ORGANIZATION NAMES(S) AND ADDRESS(S) Air Force Institute of Technology Graduate School of Engineering and Management (AFIT/EN) 2950 Hobson Way WPAFB, OH 45433-7765				8. PERFORMING ORGANIZATION REPORT NUMBER AFIT/GAE/ENG/08-01		
9. SPONSORING/MONITORING AGENCY NAME(S) AND ADDRESS(ES) AFRL/RBCA Attn: Dr. Mark Mears 2130 Eighth St WPAFB, OH 45433-7531				10. SPONSOR/MONITOR'S ACRONYM(S)		
12. DISTRIBUTION/AVAILABILITY STATEMENT APPROVED FOR PUBLIC RELEASE; DISTRIBUTION UNLIMITED.				11. SPONSOR/MONITOR'S REPORT NUMBER(S)		
13. SUPPLEMENTARY NOTES						
14. ABSTRACT This thesis developed guidance laws to optimally position a relay Micro-UAV (MAV) to provide an operator with real-time Intelligence, Surveillance, and Reconnaissance (ISR) by relaying communication and video signals when there is no line-of-sight between the operator at the base and the rover MAV performing the ISR mission. The ISR system consists of two MAVs, the Relay and the Rover, and a Base. The Relay strives to position itself to minimize the radio frequency (RF) power required for maintaining communications between the Rover and the Base, while the Rover performs the ISR mission, which may maximize the required RF power. The optimal control of the Relay MAV then entails the solution of a differential game. Applying Pontryagin's Maximum Principle yields a nonlinear Two-Point Boundary Value Problem (TPBVP). Suboptimal solutions are also analyzed to aid in solving the TPBVP which yields the solution of the differential game. One suboptimal approach is based upon the geometry of the ISR system. Another suboptimal approach envisions a stationary Rover and solves for the optimal path for the Relay. Both suboptimal approaches showed that the optimal path for the Relay is to head straight toward the midpoint between the Rover and the Base.						
15. SUBJECT TERMS Optimization, Optimal Control, Differential Games, Repeaters						
16. SECURITY CLASSIFICATION OF:			17. LIMITATION OF ABSTRACT UU	18. NUMBER OF PAGES 61	19a. NAME OF RESPONSIBLE PERSON Meir Pachter, PhD (ENG)	
REPORT U	ABSTRACT U	c. THIS PAGE U			19b. TELEPHONE NUMBER (Include area code) (937) 255-3636, ext 7247; e-mail: meir.pachter@afit.edu	

Standard Form 298 (Rev: 8-98)

Prescribed by ANSI Std. Z39-18